BIOMECHANICAL ANALYSIS OF KNEE IMPLANT WITH AND WITHOUT BONE ATTACHMENT USING FINITE ELEMENT METHOD

Naveen Chandrol

Department of Biotechnology and Medical Engineering

National Institute of Technology Rourkela

BIOMECHANICAL ANALYSIS OF KNEE IMPLANT WITH AND WITHOUT BONE ATTACHMENT USING FINITE ELEMENT METHOD

Dissertation submitted in partial fulfillment

of the requirements of the degree of

Master of Technology

in

Biomedical Engineering

by

Naveen Chandrol

(Roll No. 214BM1456)

under the supervision of

Dr. A. Thirugnanam

May 2016

Department of Biotechnology and Medical Engineering

National Institute of Technology Rourkela

Department of Biotechnology and Medical Engineering

National Institute of Technology Rourkela

May 31, 2016

Certificate of Examination

Roll Number: 214BM1456

Name: Naveen Chandrol

Title of Dissertation: Biomechanical Analysis of Knee Implant with and without Bone Attachment Using Finite Element Method

I signed, after checking the dissertation mentioned above and the official record book (s) of the student, hereby state my approval of the dissertation submitted in partial fulfillment of the requirements of the degree of *Master of Technology* in *Biomedical Engineering* at *National Institute of Technology Rourkela*. I am satisfied with the volume, quality, correctness, and originality of the work.

Prof. A. Thirugnanam

Principal Supervisor

Department of Biotechnology and Medical Engineering

National Institute of Technology Rourkela

Prof. A. Thirugnanam

Assistant Professor

May 31, 2016

Supervisor's Certificate

This is to certify that the work presented in the dissertation entitled *Biomechanical Analysis of Knee Implant with and without Bone Attachment Using Finite Element Method* submitted by *Naveen Chandrol, 214BM1456,* is a record of original research carried out by him under my supervision and guidance in partial fulfillment of the requirements of the degree of *Master of Technology* in *Biomedical Engineering*. Neither this dissertation nor any part of this work has been submitted earlier for any degree or diploma to any institute or university in India or abroad.

Prof. A. Thirugnanam

Assistant Professor

Declaration of Originality

I, *NAVEEN CHANDROL*, *214BM1456* hereby declare that this dissertation entitled " *Biomechanical Analysis of Knee Implant With and Without Bone Attachment Using Finite Element Method* " represents my original work carried out as a postgraduate student of NIT Rourkela and, to the best of my knowledge, it contains no material previously published or written by another person, nor any material presented for the award of any other degree or diploma of NIT Rourkela or any other institution. Any contribution made to this research by others, with whom I have worked at NIT Rourkela or elsewhere, is explicitly acknowledged in the dissertation. Works of other authors cited in this dissertation have been duly acknowledged under the section "References". I have also submitted my original research records to the scrutiny committee for evaluation of my dissertation.

I am acutely aware that in case of any non-compliance detected in future, the Senate of NIT Rourkela may withdraw the degree awarded to me on the basis of the present dissertation.

Date- 31 May 2016 Naveen Chandrol

NIT Rourkela

Acknowledgment

This thesis is a result of research that has been carried out at **National Institute of Technology, Rourkela**. During this period, I came across with a great number of people whose contributions in various ways helped my field of research, and they deserve special thanks. It is a pleasure to convey my gratitude to all of them.

In the first place, I would like to express my deep sense of gratitude and indebtedness to my supervisor **Prof. A. Thirugnanam** for his advice, and guidance from early stage of this research and providing me extraordinary experiences throughout the work. Above all, he provided me unflinching encouragement and support in various ways which exceptionally inspire and enrich my growth as a student and a researcher. His involvement with originality has triggered and nourished my intellectual maturity that will help me for a long time to come. I am proud to record that, i had opportunity to work with an exceptionally experienced person like him.

I am indebted to **Shreeshan Jena, Reshmi Dey, Chittaranjan Bhoi, Krishna Kumar Ramajayam, Chandrika Kumari, Tejinder Kaur** and **Veena Vyas** for their support and co-operation which is difficult to express in words. The time spent with them will remain in my memory for years to come.

My parents deserve special mention for their inseparable support and prayers. They are the people who showed me the joy of intellectual pursuit ever since I was a child. I thank them for bringing up me with care and love.

Date- 31 May 2016

NIT Rourkela Naveen Chandrol

Abstract

Degenerative arthritis is a disease that affects the line cartilage of the knee joint. It produces various injuries in the knee joint and may need a total knee replacement surgery of the affected knee with artificial components. Geometric complexity and non-linearity of the biomaterials of the knee make the logical solutions of the mechanical conduct of the knee joint difficult. In this study, 3D modeling software, SolidWorks is used for modeling of knee implant and finite element method software ANSYS 15.0 is used for numerical estimation of equivalent stress, equivalent strain, and total deformation. This study explains a human knee implant model using ANSYS 15.0 which shows multiple contact pairs working together. The objective is to find out the FEM results considering various loading state of knee implant with and without bone for various biomaterials, different meshing state of knee implant without bone for various steps. Also, this study compares these results and suggests the best biomaterial, mesh quality and time step for knee implant analysis for total knee replacement cases. A knee implant without bone static structure was able to sustain a load of 1500 N for material properties of ZrO_2 demonstrating a stable stress value of 736.52 MPa. However, a knee implant without bone transient structure could sustain a time step of 0.001 s at a medium mesh demonstrating a stable stress value of 455 MPa. It is seen that a knee implant with bone static structure was able to maintain a load of 700 N for material properties of Ti6Al6V alloy showing a stable stress value of 1036 MPa. This implant model is a geometric contact path-dependent model that includes friction between bodies, which helps in understanding it is structural, and transient mechanical behavior, thus suggesting its practical use in the field of implant replacement/ prosthesis.

Keywords - *finite element method (FEM,) SolidWorks, total knee replacement, knee joint, biomaterial.*

Contents

LIST OF FIGURES

LIST OF TABLES

Chapter 1

Introduction

1. 1 INTRODUCTION

The knee is one of the most complex and largest joints in the human body. The knee joints the shin bone (tibia) and thigh bone (femur) **(Figure 1.1)**. The smaller bone that runs alongside the tibia (fibula) and the kneecap (patella) are the other bones that make the knee joint. The knee joint is a mobile troche ginglymus (a pivotal hinge joint), which permits extension and flexion as well as a slight external and internal rotation. A complicated system of tissues provides support and mobility to the body by acting through this joint. It experiences various types of motion as a whole system, or movement of its parts, and is therefore subjected to a variety of loading conditions as a person runs, walks, or performs any other type of load-bearing activity. A set of ligaments and muscles join the three bones (the femur, the tibia, and the patella) and control the range of motion of the knee. Osteoporosis, arthritis, and related conditions are some of the most common causes of knee pain. This arthritis is one of the most common causes of knee pain (usually in elderly population) that demands surgical treatment. Further, arthritis may be classified into various types, most common of which are rheumatoid arthritis, osteoarthritis arthritis, and posttraumatic arthritis **[1-3]**.

There are essentially four separate ligaments that stabilize the knee joint. Of these, the lateral collateral ligament (LCL) and medial collateral ligament (MCL) lie on the sides of the joint. These two ligaments mainly stabilize the joint in a medial-lateral direction. In the front part of the knee joint center, there is the anterior cruciate ligament (ACL), which is a very important femur stabilizer. Directly behind the ACL is the posterior cruciate ligament (PCL) that acts complementary to the ACL. The primary function of the PCL is to prevent the tibia from sliding to the rear part of a knee **[4]**.

The knee implant commonly used in total knee replacement (TKR) surgery comprises of three components. The femoral component (top portion) replaces the bottom surface of the femur and the groove where the patella fits. The tibial component (bottom portion) replaces the top face of the tibia. The patellar component (kneecap portion) replaces the surface of the patella where it glides in the groove on the femur. The components are often anatomically shaped or contoured designs versus basic geometric shapes. They are

produced by a family in a range of sizes that can be selected during surgery to match the patient requirements **[5]**.

Various studies on a knee model have been done to evaluate stress using two-dimensional (2D) or three-dimensional (3D) finite element method (FEM). To provide an accurate representation, it is required to develop a knee implant model in three-dimensional. Over the last decade, the use of FEM as analysis tools in biomechanics and orthopedics has grown quickly. While the mathematical model of the knee joint can be useful to predict stresses and forces in the individual structure of the articulation, as well as to estimate its kinematics, validation of such models is a challenging task. It is complicated to make a computational model of the knee joint that accurately predicts the response and movement of the articulation as possible by experimental methods **[6-8]**.

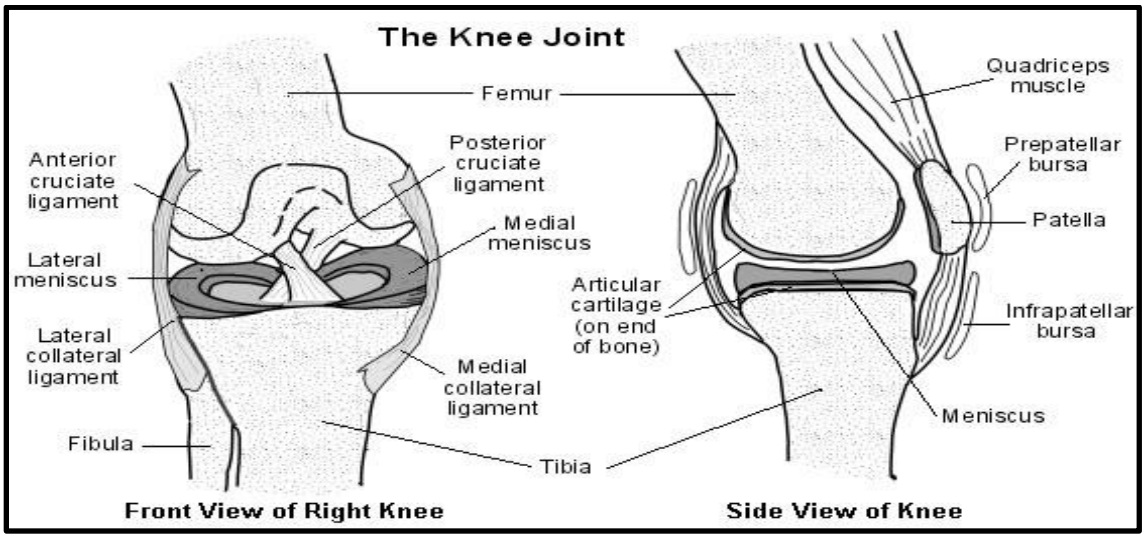

Figure 1.1 The anatomy of knee joints

1.1.1 Knee biomechanics

Biomechanics is a branch of science that applies principles studied in mechanics to the understanding of living beings. The branch focuses on understanding the complex living system with the help of analytical and experimental methods **[9]**.

Although many researchers have studied this joint in the past, the detailed mechanical behavior of the knee joint and the causes of knee injuries are not completely analyzed yet. This is partially due to unavoidable constraints in experimental studies and costs,

difficulties associated with obtaining accurate stress and strain measurements and particularly the problem to simulate certain pathological, natural or degenerative situations **[10]**.

To understand the interactive mechanical behavior of the knee joint and its structures is a complex task. The knee joint is one of the most commonly injured joint human bodies. It has to transfer body weight and is loaded by muscles forces while generating a flexible movement at the same time. One possibility for understanding 'in vivo' knee joint biomechanics is to utilize motion analysis systems **[11-12]**.

1.2 KNEE JOINT MUSCLES

The muscles of the knee joint include the quadriceps, hamstrings, and the muscles of the calf (**Figure 1.2)**. These muscles work in groups to bend, expand and stabilize the knee joint. These motions of the knee allow the body to perform such significant movements as walk, run, kick, and jump. Extending along the anterior surface of the thigh are the four muscles of the quadriceps femoris group (vastus lateral, vastus medial, vastus intermedium, and rectus femoris). These largest muscles originate in the femur and insert on the tibia bone. Contraction of the quadriceps group extends the leg at the knee joint and flexes the thigh at the hip joint.

Three sets of muscles (quadriceps, popliteus, and hamstrings) allow for balance, movement, and stability at the knee joint. The popliteus (a small muscle at the back of the knee joint that aids in bending the knee joint and in the rotation of the lower leg) muscle at the back of the leg unlocks the knee joint by rotating the femur on the tibia, allowing flexion of the knee joint. The quadriceps (a muscle having four heads, especially the large extensor at the front of the thigh) femorus muscle group (vastus medius, rectus femoris, vastus intermedius and vastus lateral) crosses the knee via the patella and acts to stretch the leg. The hamstring muscles refer to any one of the three posterior thigh muscles (biceps femoris semimembranosus, and semitendinosus) that make up the borders of space behind the knee joint. The hamstring muscles bend (flex) the knee joint. While all but the short head of biceps femoris stretch (straighten) the hip joint. The three 'true' hamstrings cross both the hip joint and the knee joint and are, therefore, involved in knee joint flexion and hip joint extension. The short head of the biceps femoris crosses only

one knee joint and thus is not involved in hip joint extension. The hamstring plays a major role in many daily activities such as running, walking, jumping and controlling particular movement in the trunk. In walking, they are most famous as an antagonist to the quadriceps in the deceleration of knee extension. The vastus lateral is on the lateral side of the femur bone (on the outer aspect of the thigh). The vastus medial is on the medial side of the femur bone (on the inner part thigh). The vastus intermedium lies between vastus medial and vastus lateral on the front of the femur bone (on the top or front of the thigh), but deep to the rectus femoris. All four parts of the quadriceps muscle ultimately insert into the tibial tuberosity of the tibia bone **[3, 13]**.

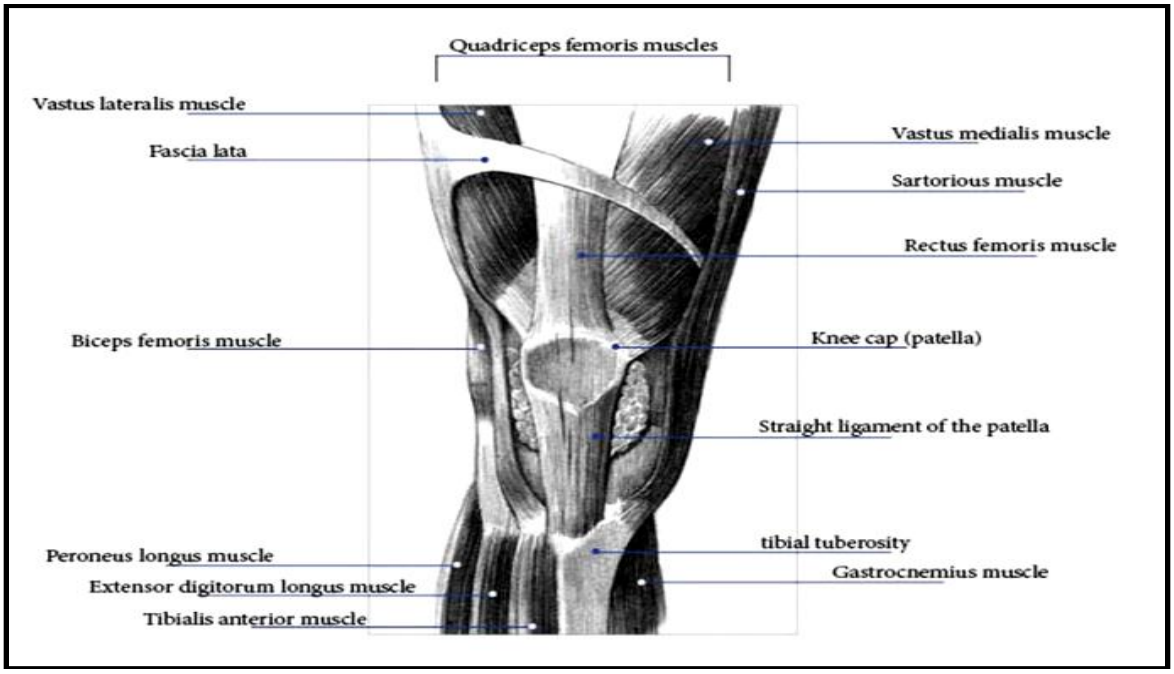

Figure 1.2 The anterior view of knee joint muscles [3]

1.2.1 Knee joint mechanical planes and movement

Knee joint movement

An axis is a line around which motion occurs. Axis is related to planes of reference, and the cardinal axes are oriented at a right angle to one another. This is expressed as a 3D coordinate system with x, y, and z used to mark the axes **(Figure 1.3)**.

The significance of this coordinate system is in defining or locating the extent of the types of movement possible at each joint rotation, translation, and curvilinear motion. All

movements that occur about an axis are considered rotational, whereas linear movement along an axis and through a plane is called translational movement. Curvilinear motion takes place when a translational movement accompanies rotational movements. The load that produces a rotational movement is called torsion. Force that provides a translational movement is known as a shear or axial force. During activities of daily living (ADL), sports and exercise, the movement usually occurs in more than one plane at a given joint. Understanding axis and planes of the body is useful for describing the major body instrumental and movements when designing effective exercise programs **[14]**.

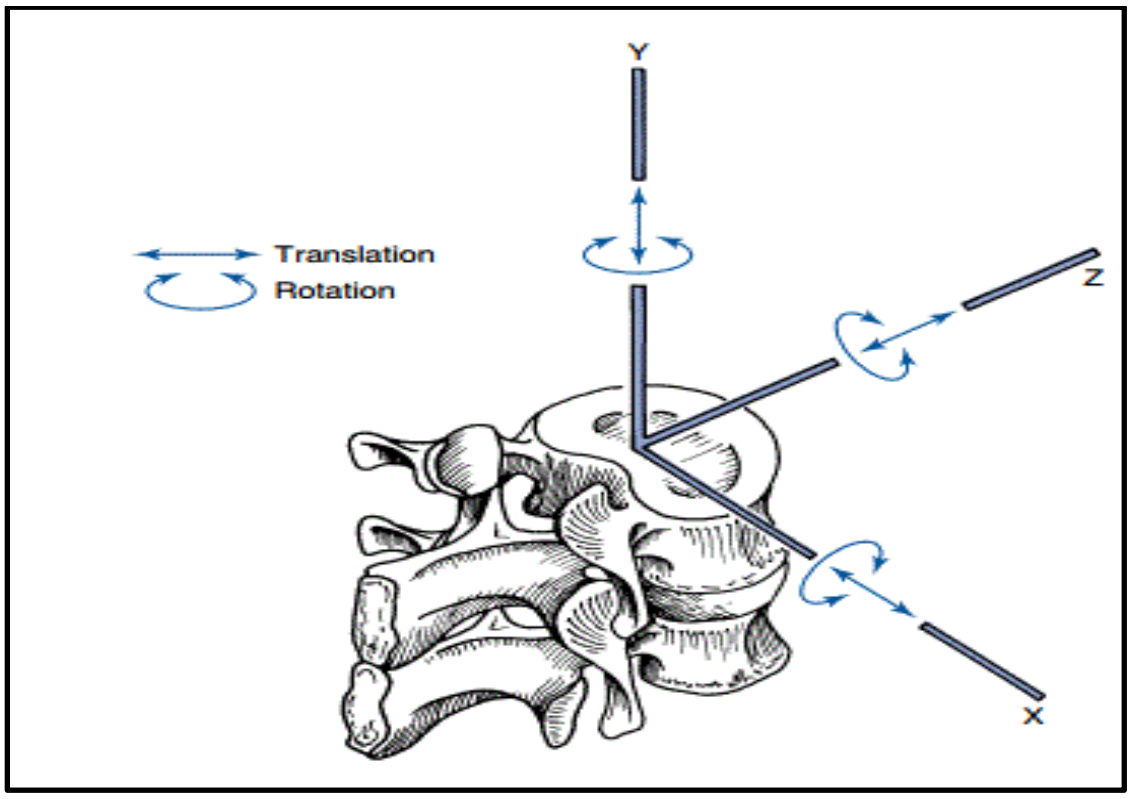

Figure 1.3 A 3D coordinate system with the rotational and translational movements [14].

Mechanical planes

It is also necessary to delineate the specific body planes of reference since they will use to describe the structural position and directions of functional movement. The sagittal plane is perpendicular and extends from front to back or posterior from anterior. The median sagittal plane also called the mid-sagittal. Movements of flexion and extension take place in the sagittal plane. The plane cuts the body into left and right halves **(Figure**

1.4 (a)). The coronal plane is perpendicular and extends from side to side. It may also be mentioned too as the frontal plane, and it separates the body into the posterior and anterior component. Movements of abduction and adduction (lateral flexion) take place in the coronal plane **(Figure 1.4 (b)).** The transverse plane is a horizontal plane and cuts a structure into lower and upper component. Movements of medial and lateral rotation take place in the transverse plane **(Figure 1.4 (c)) [2, 15-17]**.

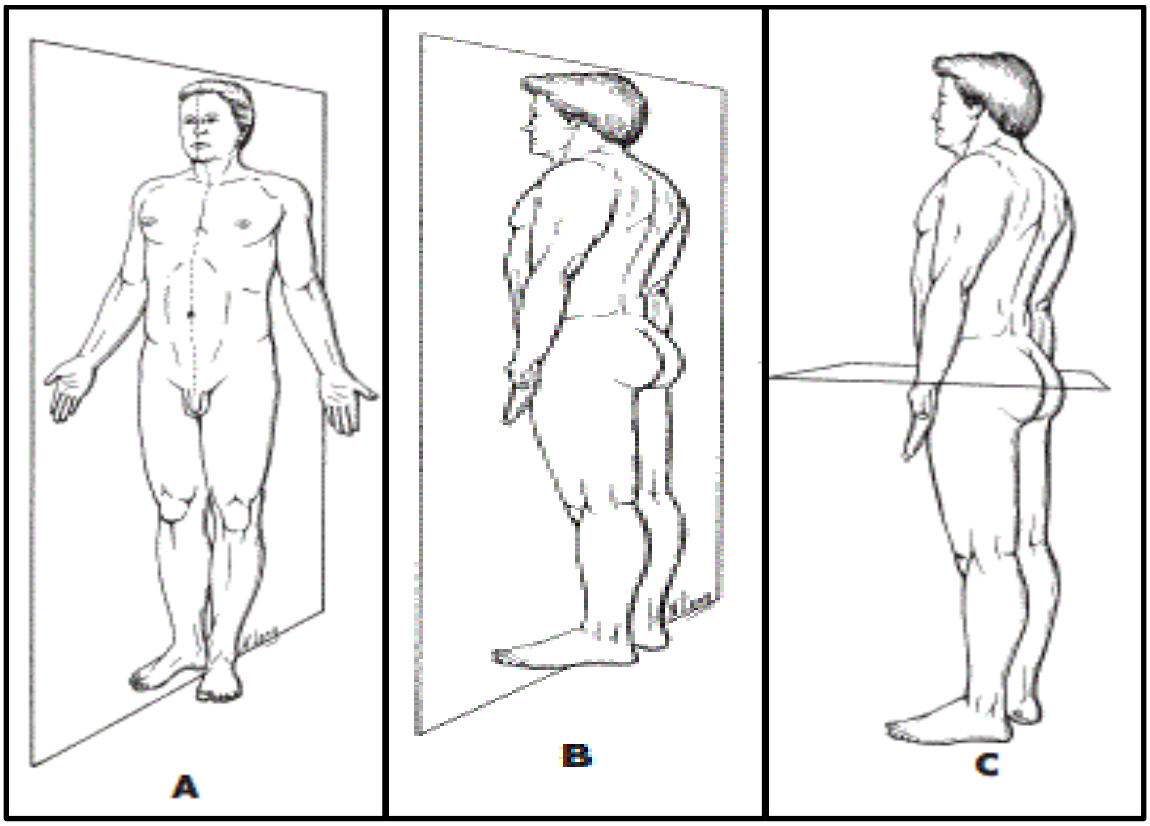

Figure 1.4 Functional body plane (a) mid-sagittal plane (b) coronal plane and (c) transverse plane [14].

1.3 KNEE PROSTHESIS

In the area field of reconstructive/rehabilitative medicine, prosthetics are the artificial devices that replace diseased or damaged body parts. These devices can be used on the exterior of the body or can be surgically implanted. Prosthetic constructs are a combination of one or more kind of materials and may serve either a cosmetic or functional purpose or both.

The knee implant prosthesis is an artificial device that is used to replace the natural biological joint articulation by a set of metallic or nonmetallic materials (or a combination) to reduce the pain in the joint. Typically a knee implant may consist of four parts namely **(Figure 1.5)** the femoral cup, tibia insert, the articulating/lubricating layer and the patellar region.

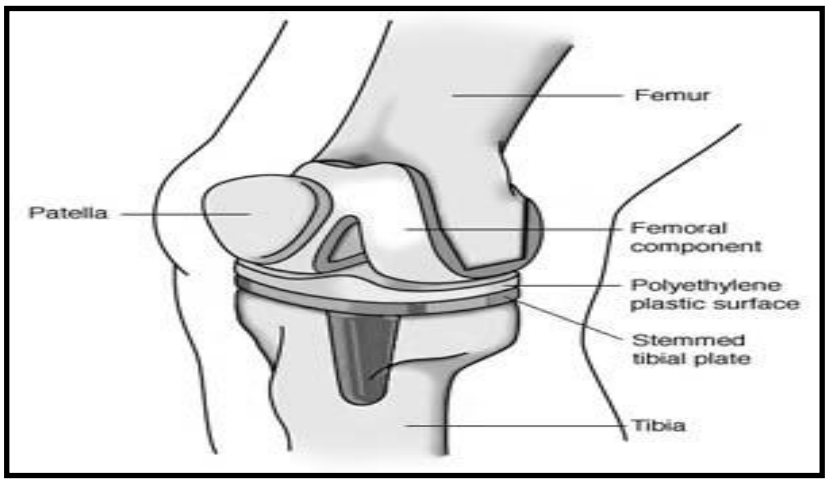

Figure 1.5 The anatomy of knee implant

1.3.1 Knee implant design criteria

The following basic criteria must be kept in mind while designing knee implant prosthesis for clinical use

1. They must be biocompatible and can be placed in the body without creating any rejection response.
2. They should be strong enough to take loads higher than the body weight and should be sufficiently flexible to bear stress without reaching failure.
3. The surfaces of the tibia and femoral insert should be able to move smoothly over each other with minimum friction. An intermediate layer of the lubricating substance may be used.

Metallic alloy has been the materials of choice since the start of orthopedic surgical treatment. Orthopedic materials must fulfill the mechanical, biological and physical necessities of their proposed utilization as mentioned above. The knee joint gets variable loads in different moving conditions. The materials used as biomaterials may consist of

metals, composite, ceramics, and polymers. Out of these cobalt-chromium alloy, titanium alloy, stainless steel and ultra high molecular weight polyethylene (UHMWPE) are the most commonly used biomaterials **[1]**.

1.4 KNEE REPLACEMENT PROCEDURE

Surgical techniques differ depending on the patient's needs and the physician's approach. Usually, the following approach is adopted to perform a TKR surgery.

- The patient's vital signs are checked to make certain heart rate, blood pressure, oxygenation level, and body temperature are normal, and then surgery can commence. A mark is made on the knee joint undergoing surgery.
- Anesthesia is then administered to the patient. He may receive general anesthesia or be given a local anesthesia to prevent sensation from the waist down along with a relaxant **(Figure 1.6 (a))**.
- The physician makes a cut down the middle of the knee joint about 7 to 10 inches long, and then cuts through deeper tissue, including the quadriceps tendon, and flips over the kneecap to access the tibia and femur. Alternatively, some physicians make smaller cuts and use minimally invasive techniques for total knee replacement **(Figure 1.6 (b))**.
- To improve the physician's ability to access to the joint, the knee is flexed to 90˚ **(Figure 1.6 (c))**.
- The physician uses a bone saw to remove the arthritically damaged areas from the top of the tibia and the bottom of the femur. Each bone is reshaped to fit exactly to its new prosthesis. Because these cuts must be precise, the physician uses either a metal jig or computer assistance to line up the cuts. **(Figure 1.6 (d))**.
- A physician may resurface the back of the kneecap, or patella, and attach an implant. A polyethylene component may be included with facilitate the patella's gliding against the new knee joint. **(Figure 1.6 (e-f))**.
- Components are attached to the tibia, the femur, and patella. The implant components are appended to the bone will depend on what type of component is used. Artificial knee replacements may be classified into two basic type's cementless prosthesis and cemented prosthesis. Cemented prosthesis is held in place by a kind of epoxy cement

for fixation. The cementless prosthesis has a rough, porous surface intended for bone to grow and attach the prosthesis to the bone.

- A flexible cushion made of polyethylene is attached on top of the new tibia surfaces. This spacer acts as a shock absorber between the two new prosthetic surfaces **(Figure 1.6 (g))**.
- The leg is extended and flexed to test the adaptation of the components and the new knee range of motion. **(Figure 1.6 (h))**.
- The physician straightens the knee joint to allow the cement, components, and bone to bond mutually as the bone cement, polymethylmethacrylate (PMMA) is fast acting. The physician will repair any deep tissue that was cut during surgery and then stitches the skin at the incision **[18-20]**.

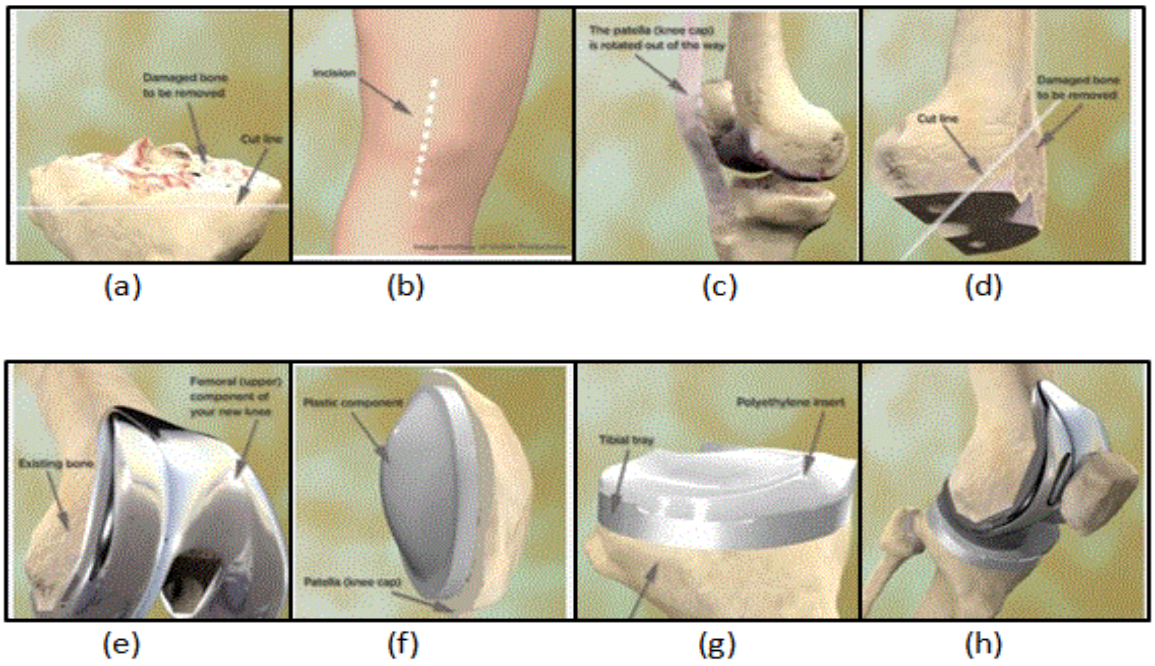

Figure 1.6 Total knee replacement complete procedure (a) bone is reshaped to fit exactly its new prosthesis, (b) a cut down the middle of the knee joint about 7 to 10 inch long, (c) knee is flexed to 90 degrees, (d) bone is reshaped to fit exactly its new prosthesis, (e,f) attached the femoral component and patella, (g) a flexible cushion made of polyethylene is attached, (h) leg is extended.

Chapter 2

Literature review

2.1 INTRODUCTION

One of the current challenges faced by new orthopedic implants is to produce the component of high strength, resistance to fatigue, and low production cost. Technologies have been the focus of major scientific and policy discussion since the failures of articular surface replacement and large head size metal on metal articulation in total knee replacement were brought to light. Among all knee implant is a process where difficult to produce shapes, can be formed with higher mechanical properties and near net shape production can be achieved **[13, 21].**

2.2 STUDY OF BIOMATERIAL

The replacement knee joint is comprised of stems and a flat metal plate implant in a tibia. A contoured metal implant and a polyethylene bearing surface match around the point of a femur. The use of component made from polyethylene and metals allow for best articulation (or joint mobility) between the combined surfaces with little wear. The knee implant has a flat bearing, wear problem is less than in a hip implant that has a very high bearing **[22].**

Stainless steel alloy - Stainless steel is not usually used in knee replacement implant due to limited capability to withstand corrosion in the human body in long term use. It is more suited to being used as temporary such as fracture screws and plates.

Cobalt chromium alloy - Cobalt Chromium alloy is tough, hard, biocompatible corrosion resistant metal. Along with titanium, cobalt chrome is one of the most used metals. Although the percentage of patients having allergic reactions related to the use of cobalt chromium alloy is very limited, one area of concern is the issue of tiny particles (metal ions) that may release into the body as a result of joint movement. These particles can sometimes cause reactions in the human body, especially in the case of those patients who have the allergy to primary metals like nickel.

Titanium and titanium alloy - Pure titanium used in implant where higher strength not necessary. For example, the pure titanium is sometimes used to produce fiber metal. A Layer of metal fibers bonded to the surface of an implant that allows cement to better bond to the implant for greater fixation and enable the bone to grow into the implant. Titanium alloy is biocompatible in nature. They ordinarily contain amounts of aluminum

and vanadium in addition to titanium. The most used titanium alloy in is Ti6Al4V. Titanium alloy and titanium have excellent corrosion resistance, making them inert biomaterial (which means they will not change after inserted in the body).Titanium and its alloy have lower density compared to other material used. Additionally, the elastic nature of titanium alloy and titanium is less than that of the other metals used in the knee implant. The titanium implant acts more like the first joint, and as a result, the chance of some complications like atrophy and bone resorption is overcome.

Polyethylene (UHMWPE) - The polyethylene is renowned as patella and the tibial component in the knee replacement. The use of ultra high molecular weight polyethylene (UHMWPE) and ultra highly cross-linked polyethylene (UHCLPE) reduces even the minimal wear enabling the knee implant to last for a much longer time.

Zirconium oxidized - It is a new material used in knee implant since 2001. It is a transformed metal alloy that has a ceramic bearing surface. It contains niobium alloy and zirconium that was oxidized to convert the surface of the material into zirconium ceramic. The real thing of this metal alloy is that just the surface has changed, so the rest of the implant component is a high soft metal. Although it is twice as hard as cobalt chromium alloy, it provides half the friction thus performs with more top quality and lasts for a longer time.

Table 2.1 Yield and permissible strength for biomaterial [23]

Material	Yield strength (MPa)	Allowable stress (MPa)
Ti6Al4V alloy	900	300
Co-Cr alloy	525	175
316L SS alloy	240	80-120
ZrO_2	900	300

2.3 STUDY OF PREVIOUS WORK

The adaptive bone remodeling process could be discussed mathematically and simulated in a computer model, integrated with the finite element method. In the model described by **H. Weinans**, trabecular and cortical bone are depicted as continuous materials with variable density **[24]**. The remodeling rule applied to simulate the reconstruction process in each element individually is, in fact, an objective function for an optimization process, about the external load. A constant, preset value for the strain energy per unit bone mass could be obtained by density adaptation. If a component in the structure could not achieve that, it either turns to its maximal density (cortical bone) or resorbs completely. A discontinuous patchwork was found as a general solution. For a two-dimensional proximal femur model, this mishmash showed similarity with the density distribution of a real proximal femur. The discontinuous end configuration was dictated by the nature of the differential equations describing the remodeling process. This process could be considered as a nonlinear dynamical system with many degrees of freedom, which behaves divergent about the objective, leading to many possible solutions. The correct solution was dependent on the parameters in the remodeling rule, the load, and the initial conditions. The feedback mechanism in the process was self-enhancing; denser bone attracts more strain energy, whereby the bone becomes even thicker. It was suggested that this positive feedback of the attractor state (the strain energy field) creates order in the end configuration. Also, the process ensured that the discontinuous end configuration was a structure with a relatively small mass, perhaps a minimal mass structure, although this was no explicit objective in the optimization process. The hypothesis was that trabecular bone a chaotically ordered structure which could be considered as a fractal, with optimal mechanical resistance and minimal mass, of which the actual morphology depended on the local (internal) loading characteristics, sensor cell density and degree of mineralization. The ligaments of the knee joint consist of fiber bundles with variable, lengths, orientations and mechanical properties. This structure was too often seen as structures, which are either stretched or slack during knee joint motions.

T.J. A. Mommersteeg introduced a new structural concept of the ligaments of the knee joint. The multi-bundle ligament structures were considered as non-uniform mechanical

properties and zero force-length. For this purpose, characteristics of a human the knee joint were compared as measured in a predicted and experiment in a model simulation examine. In this experiment, the valgus-varus and posterior-anterior laxities of a knee joint specimen containing the ligaments and the articular surfaces only were determined. From this knee joint, mechanical and geometric parameters were derived to supply the parameters for a 3D quasi-static knee joint model. These parameters included the 3D insertion points of bundles, defined in the four major knee ligaments, the mechanical properties of this ligament, as functions of their relative insertion orientations and, a 3D representation of the articular surface. In this model, the experiments were simulated. If knee model experimental and predictions results agree, then the multi-bundle ligament models were validated, at least on their functional role in anterior-posterior and varus-valgus loading of the joint. The model described the laxity characteristics in the valgus-varus rotation and posterior-anterior translation of the cadaveric knee joint Specimen reasonably well. Both display the same patterns of carelessness changes during knee flexion. From model and experiment comparison, it was concluded that the proposed structural representation of the ligaments and their mechanical property distribution seem to be valid for studying the posterior-anterior and valgus-varus characteristics of the human knee joint **[25]**.

Stephen J. Piazza developed 3D dynamic model of the patellofemoral and tibiofemoral articulations was created to predict the motions of knee implant during a step up activity. The purpose behind this novel mathematical model of knee development is to incorporate the design into a whole body, forward dynamic, musculoskeletal simulation of a step up the task. Prosthetic knee kinematics defined by integration of dynamic equations of motion subject to forces generated by ligaments, muscles, and contact at both patellofemoral and tibiofemoral articulations. The simulation reproduced experimentally measured flexion-extension angle of the knee, but translations at the tibiofemoral articulations were larger during the step up analysis task than those reported for patients with total knee replacements **[26]**.

Jiann Jong Liau investigated the effect of malalignment on stresses in polyethylene component of total knee prostheses using 3D finite element analyses. At the ideal contact

alignment, many biomechanical studies examined the stresses in polyethylene tibial component. The effect of malalignment on stresses in polyethylene tibial component was not investigated extensively. A three-dimensional finite element analysis calculated contact stress and von Mises stress in the polyethylene tibial component subjected to a compressive load, and the malalignment situations were simulated. The greatest increases in contact stress and von Mises stress occurred in the high conformity flat on the flat design of knee prosthesis under the severest malalignment condition. Therefore, the high compliance curve on curve design of knee prosthesis had the minimal risk of polyethylene wear under malalignment conditions **[27]**.

K.E. Moglo reviewed the extent of coupling between the posterior and anterior cruciate ligaments as well as the part of the posterior cruciate ligament in the knee joint response under anterior femoral forces at different flexion angles. A developed finite element model of the tibiofemoral joint is used to perform nonlinear elastic static analyses. The structural properties of the posterior cruciate ligament after an injury altered not only the function of ligament itself but also the other intact cruciate ligament and the entire joint. The model consists of two bony type structure and their menisci articular cartilage layer and four principal ligaments. Fewer than 100 N anterior femoral loads at different flexion angles from 0 degrees to 90 degrees, kinematic, forces in ligament and contact forces in the fully unconstrained joint were computed in the intact case and following alterations in the joint ligament. Collateral ligaments were the primary structure to resist the strength at full extension under 100 N posterior femoral loads with a modest contribution from the anterior cruciate ligament. With joint flexion up to 90 degrees, however, force in the posterior cruciate ligament substantially increased whereas that in collateral ligament diminished. An odd coupling was found between the posterior cruciate ligament and the anterior cruciate ligament in flexion. A structural alteration in one of them significantly influenced the mechanical role of type ligament not just the one affected **[18]**.

.

Chapter 3
Materials and Methods

3.1 MATERIAL PROPERTIES

Commonly used biomaterials for knee implant fabrication include titanium alloy (Ti6Al4V alloy), cobalt chromium alloy (Co-Cr alloy) and stainless steels alloy (316L SS alloy). In polymers, ultra high molecular weight polyethylene is most usually used biomaterial, used for providing a lubricating layer between the femoral and tibial implant. In this study for performing a biomechanical investigation of the knee implant assembly with bone and without bone the following materials have been assigned.

(a) Ti6Al4V alloy,

(b) Co-Cr alloy

(c) 316L SS alloy

(d) ZrO_2 (oxidized zirconium)

(e) UHMWPE (ultra high molecular weight polyethylene)

The properties of materials used in this study have been shown in **Table 3.1** below.

Table 3.1 Mechanical properties of biomaterial [22-23, 28-30]

	Density (kg/m^3)	**Young Modulus (Pa)**	**Poisson Ratio**	**Bulk Modulus (Pa)**	**Shear Modulus (Pa)**	**Tensile Yield Strength (Pa)**	**Tensile Ultimate Strength (Pa)**
ZrO_2	6040	2.1×10^{11}	0.3	1.75×10^{11}	8.07×10^{10}	9×10^{8}	2×10^{9}
Ti6Al4V	4430	2.3×10^{11}	0.34	2.42×10^{11}	8.56×10^{10}	8.8×10^{8}	9.5×10^{8}
Co-Cr	8300	1.15×10^{11}	0.3	9.5×10^{10}	4.4×10^{10}	2.8×10^{8}	9.7×10^{9}
316L SS	8000	1.97×10^{11}	0.3	1.64×10^{11}	0.75×10^{11}	6.12×10^{8}	6.3×10^{8}
UHMWPE	930	6.9×10^{8}	0.29	5.47×10^{8}	2.67×10^{8}	2.1×10^{7}	4.8×10^{7}
Bone	1550	179×10^{6}	0.4	298.33×10^{6}	$639.\times10^{6}$	135×10^{6}	205×10^{6}

3.2 OBJECTIVES

1. To perform multisets of static analysis of knee implant with and without the bone.

- Grid independence test.
- Time step independence test.
- Stress, strain and deformation analysis (static).

2. To input gait parameter into FEM and study equivalent stress, equivalent strain and total deformation.

- To record gait using 3D motion analysis system.
- To use the output of the movement analysis system as an input for FEM analysis.
- To obtain the output of the motion analysis system.
- Importing motion analysis data into FEM.
- Stress, strain and deformation analysis (transient).

3.3 Modeling of knee joints in CAD

3.3.1 Using SolidWorks 2012

SolidWorks is CAD software used mainly for mechanical design automation application that lets designers quickly sketch out concepts, experiment with features and dimensions, and produce models and complete sketch. The geometry of prosthesis has a significant impact on its performance and hence there is a need for adopting the standard method to model the prosthesis. SolidWorks is a computer graphics system for modeling different mechanical design and for performing similar designs and manufacturing operations, and design. SolidWorks is a feature based parametric solid model system with several extensive development and manufacturing applications **[31-32]**.

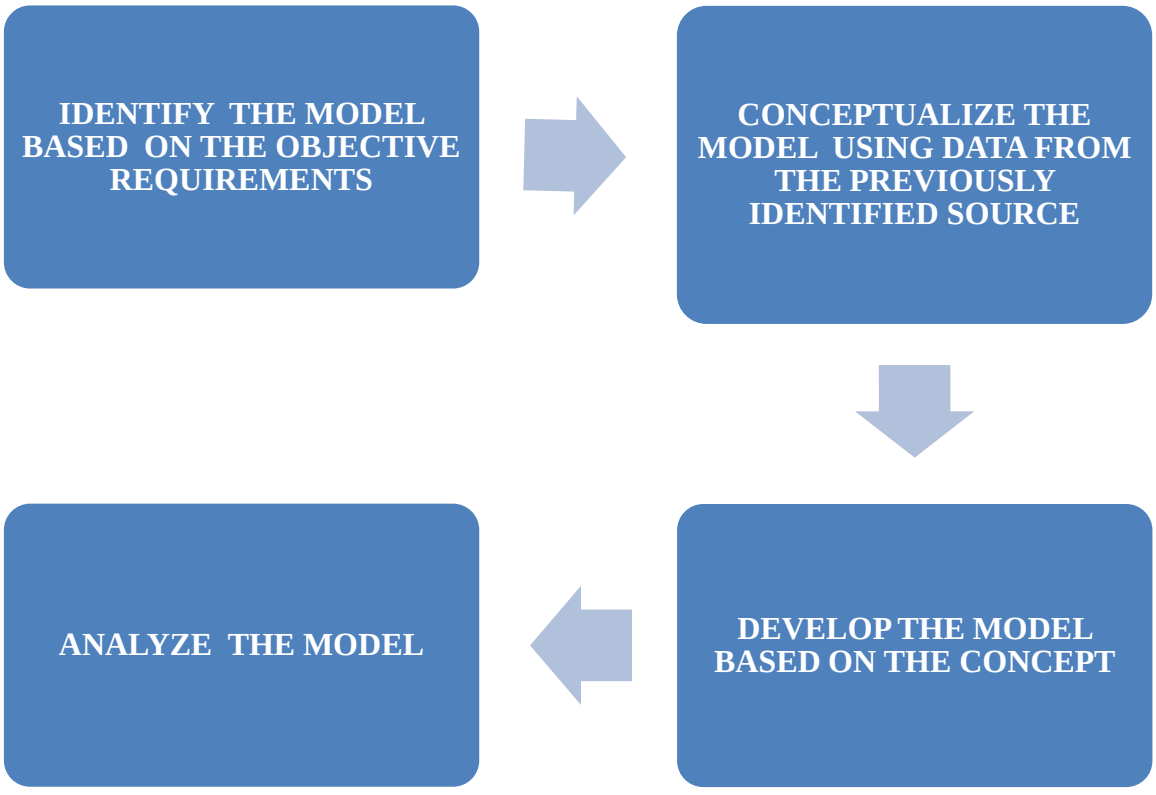

Figure 3.1 Designing process in SolidWorks

3.3.2 Designing knee implant model without bone using SolidWorks

There are three components in a designed model of total knee replacement implant which is a femoral component, tibial pin, and the base plate. Femoral component made up of metal which curves around the end femur **(Figure 3.3)**. It is inserted in such a manner so that the kneecap can move smoothly up and down during knee flexion and extension. The top surface of the tibial part is made of a flat metal platform and should have good tensile strength and a high durability **(Figure 3.4)**. For the stability of the implant the stem of the component inserted into the center of the tibia bone **(Figure 3.5)**. Patella back surface component is a dome-shaped structure, and the patellar component is ignored in this analysis.

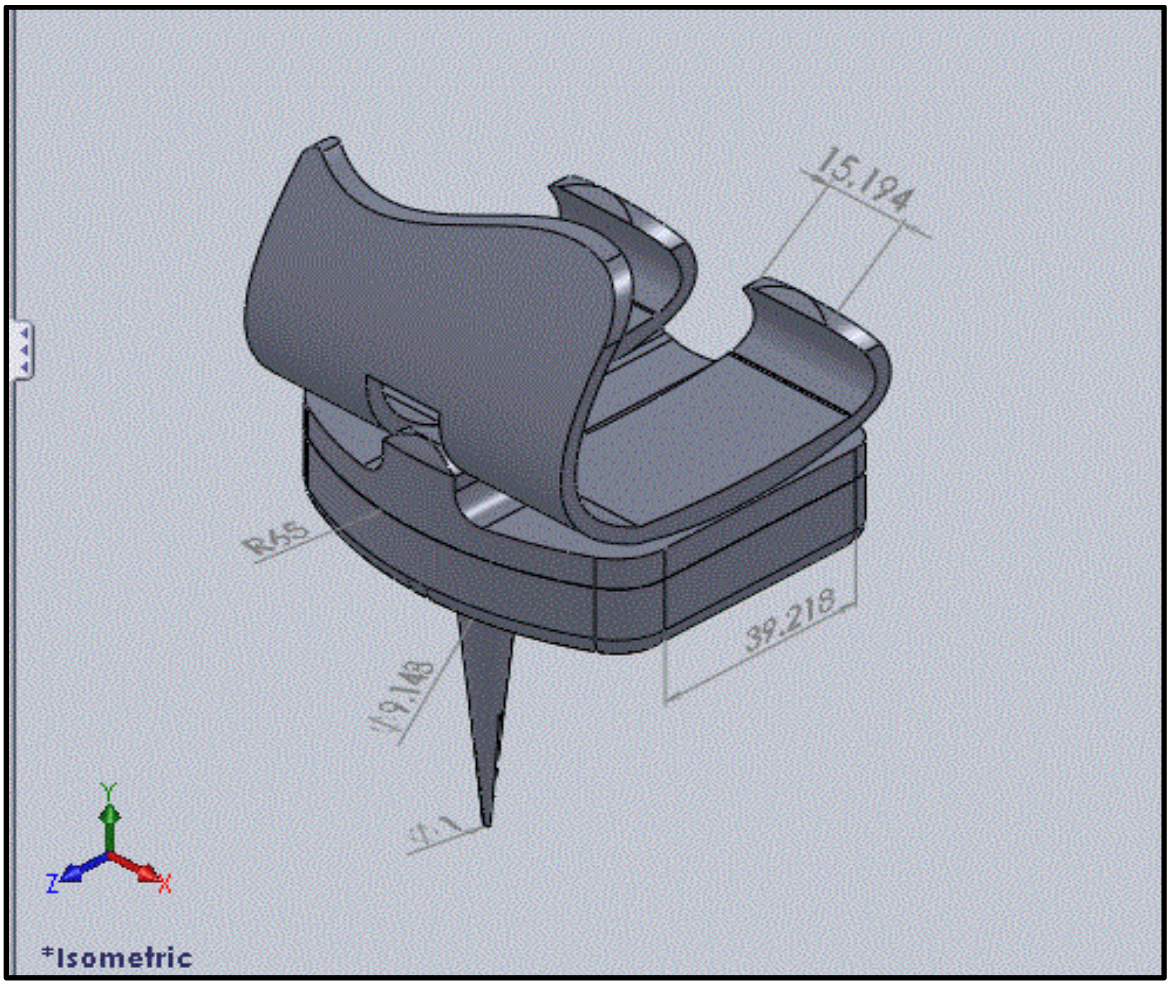

Figure 3.2 Design of knee implant in SolidWorks

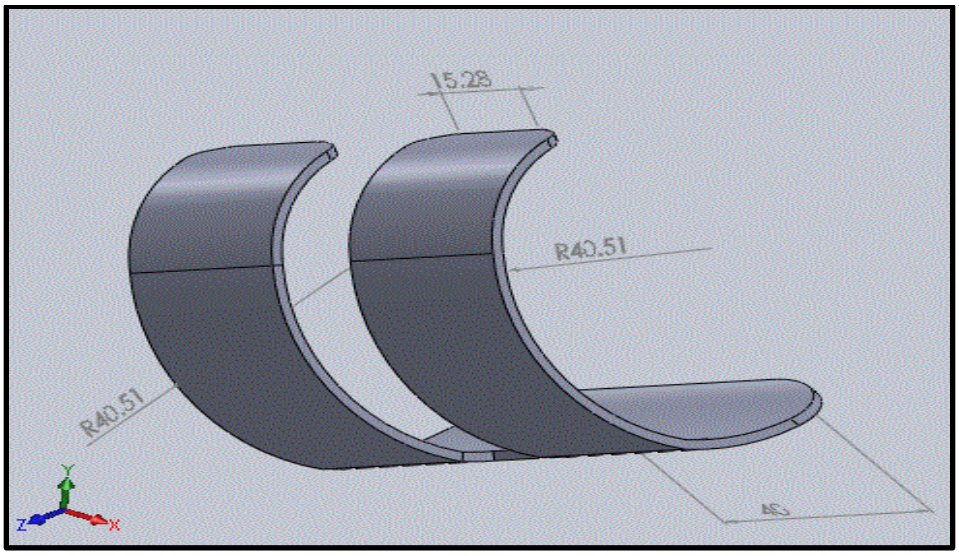

(a)

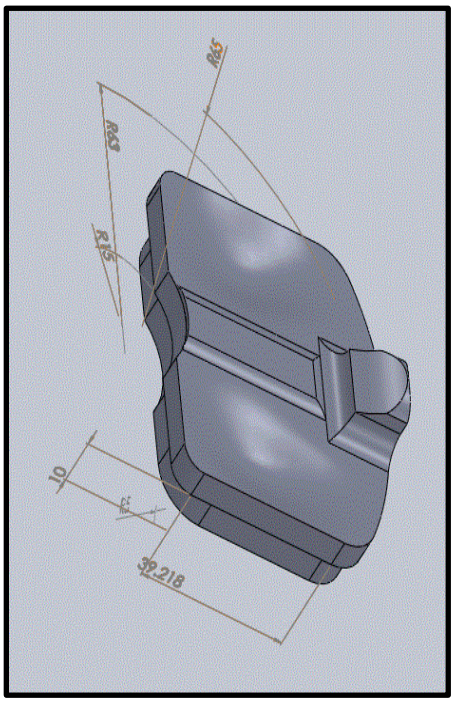

(b)

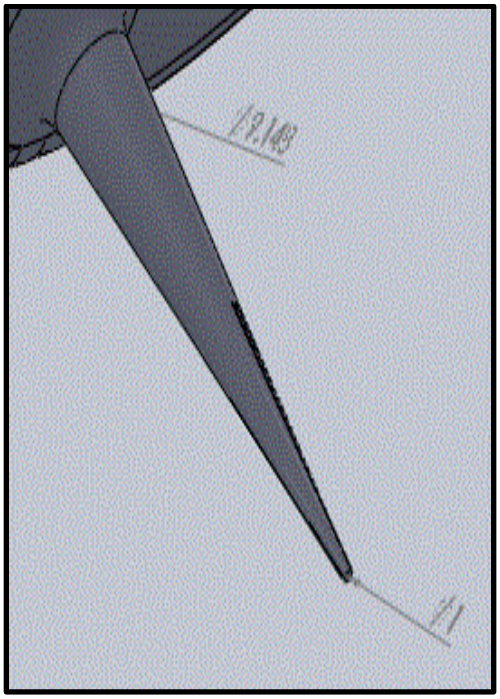

(c)

Figure 3.3 Design knee implant model in SolidWorks (a) femur cover (b) base plate (c) tibia pin

3.3.3 Design in knee implant model with bone using SolidWorks

This study built up the knee joint model using CT scan data. The database maintained includes complete CT images of the whole human body in slices. The combined 2D CT image was converted to a 3D image using ITK snap which is capable of handling CT data. The 3D image was cleaned using meshlab. Then it was converted into SolidWorks file format (.sldprt) in the next step. The basic methodology for retrieval of anatomical structures was outlined in the shows (**Figure 3.6)**. The modeling process of the hard tibia and femur bone with knee implant **[21, 33]**.

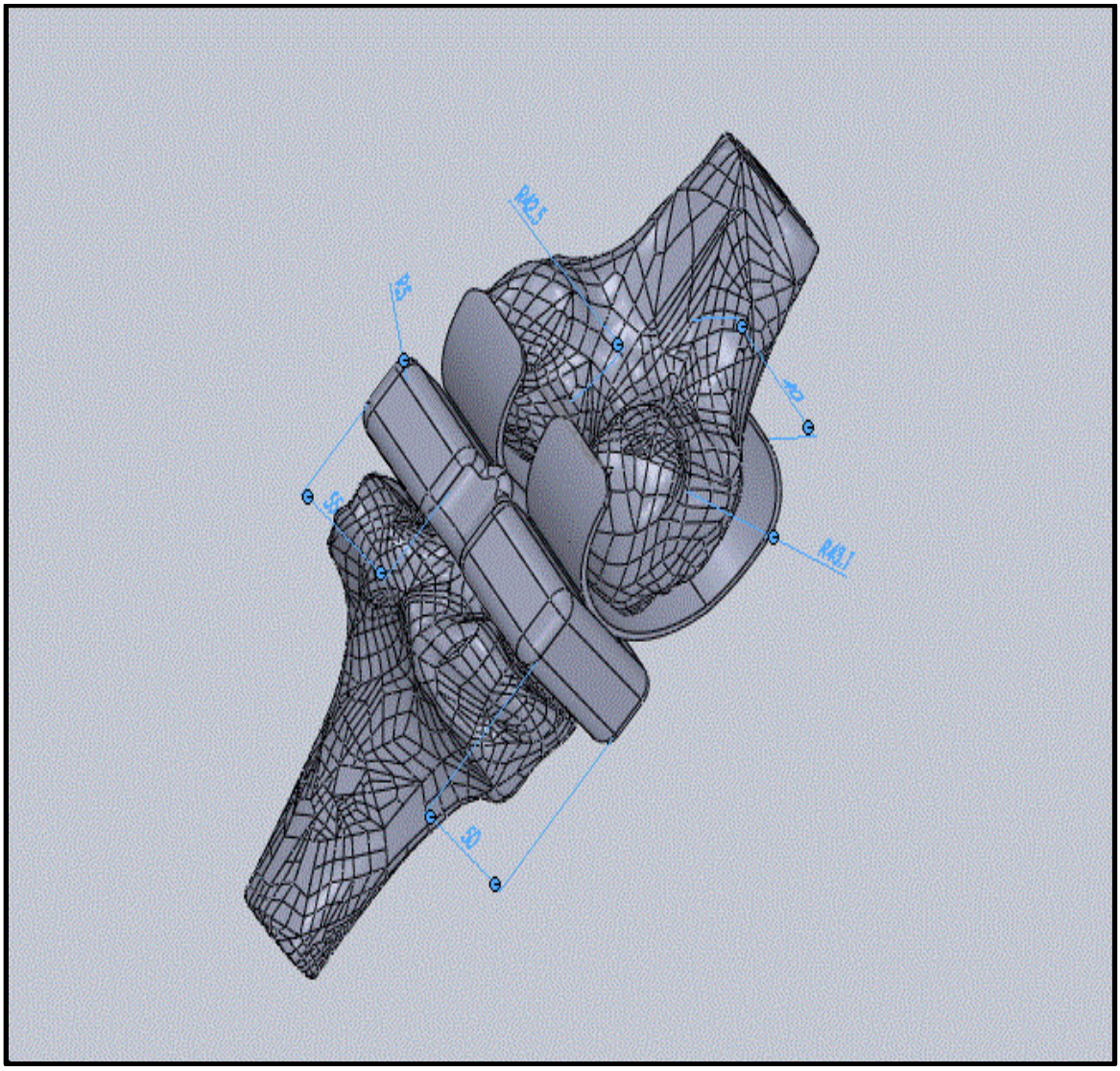

Figure 3.4 Design of knee implant with bone in SolidWorks

3.4 ANSYS (FINITE ELEMENT ANALYSIS)

The knee implant was then imported into an ANSYS 15.0 to perform the analysis. The preprocessing steps involved importing engineering material property, loading data of some commonly used alloy for making the femoral and tibial parts of the implant. Material properties of different models were defined as homogenous, isotropic with linear behavior and they were described by young's modulus and poison's ratio values. Post processing tools for ANSYS workbench can be used to generate meaningful graphics, animations, and reports that make it easy to convey the results of static and transient analyses **[4, 21, 33-37]**.

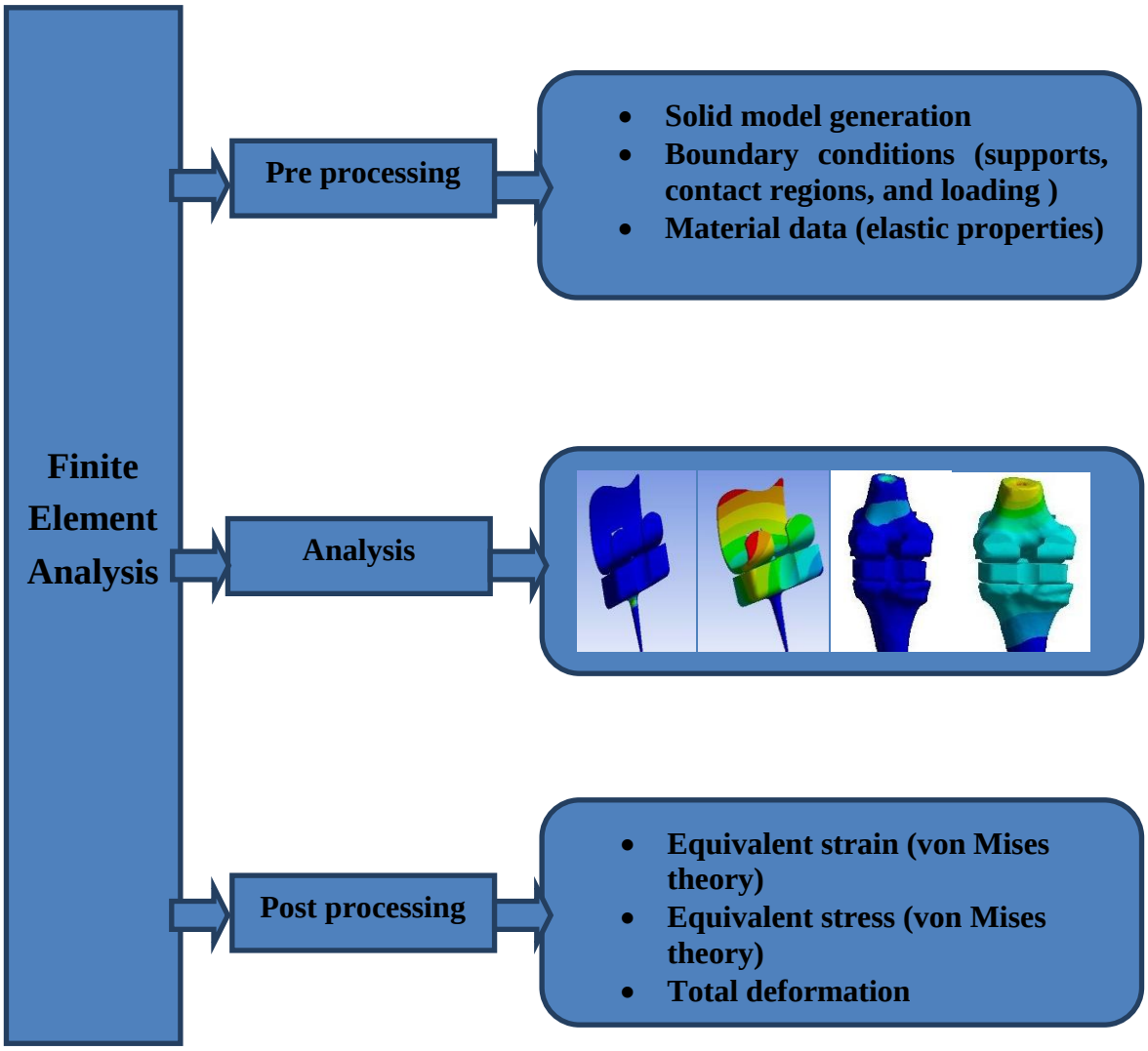

Figure 3.5 Major steps of finite element analysis (FEM)

3.4.1 Finite element analysis of a knee implant model using static loading

Preprocessing conditions

(i) A fixed support was applied at the conical base of tibia bone insert.

(ii) A load of 700 N, 1000 N, 1500 N and 2000 N was applied in the downward direction, acting on the top face of the femoral bone insert.

Analysis

Under solution information, the results obtained after the finite element analysis contained the values as well as color contour plots for total deformation, equivalent strain, and equivalent stress. The results of the analysis are shown in the following sections.

Post processing condition

(i) After obtaining one set of solutions load were changed.

(ii) After obtaining one set of solutions, material was changed.

3.4.2 Finite element analysis of a knee implant model using transient loading

Preprocessing conditions

(i) A fixed support was applied at the conical base of tibia insert.

(ii) Loads of 700 N, 1000 N, 1500 N and 2000 N were applied in the downward direction, acting on the top face of the femoral insert.

Analysis

Under solution information, the results obtained from the finite element analysis contained the values as well as color contour plots for total deformation, equivalent strain, and equivalent stress. The results of the analysis are shown in the following sections.

Post processing condition

(i) After obtaining one set of solutions, the mesh sizing was changed.

(ii) After obtaining one set of solutions, time step was changed.

3.4.3 Finite element analysis of a knee implant model with bone using static loading

Preprocessing conditions

(i) A fixed support was applied at the conical base of tibia bone insert.

(ii) A load of 700 N, 1000 N, 1500 N and 2000 N was applied in the downward direction, acting on the top face of the femoral bone insert.

Analysis

Under solution information, the results obtained after the finite element analysis contained the values as well as color contour plots for total deformation, equivalent strain, and equivalent stress. The results of the analysis are shown in the following sections.

Post processing condition

(i) After obtaining one set of solutions load were changed.

(ii) After obtaining one set of solutions, material was changed.

Chapter 4
Results and Discussion

4.1 RESULTS OF STATIC ANALYSIS OF KNEE IMPLANT

4.1.1 Static analysis of Co-Cr alloy based knee implant without bone

In this case, the preprocessing and input information is same as mentioned earlier. The simulation was performed, and the maximum and minimum values of the total deformation, equivalent strain, and equivalent stress were recorded and tabulated along with their images. In the current analysis, material conditions were applied Co-Cr alloy. A load of 700 N, 1000 N, 1500 N and 2000 N was used in this static analysis. **Table 4.1** represents all analysis of knee implant model without the bone. The current analysis Co-Cr alloy material conditions were applied. In the solution part, the maximum values of knee implant model were found. The materials along with their maximum response are discussed in this section. Maximum equivalent stress value was recorded in the 19.6×10^{7} Pa condition. Maximum equivalent strain value was found out in the 5.4×10^{-3} m/m condition. Maximum total deformation value was recorded in the 14.83×10^{-4} m condition.

Table 4.1 Results of static analysis knee implant without bone using Co-Cr alloy

	Eq. Stress (Pa)		**Eq. Strain (m/m)**		**Total deformation (m)**	
LOAD	**Maximum Value**	**Minimum Value**	**Maximum Value**	**Minimum Value**	**Maximum Value**	**Minimum Value**
700 N	3.4371×10^{8}	5.82×10^{-1}	2.068×10^{-3}	2.114×10^{-18}	6.9205×10^{-5}	0
1000 N	4.9101×10^{8}	8.31×10^{-1}	2.873×10^{-3}	4.560×10^{-12}	9.8864×10^{-5}	0
1500 N	7.3×10^{8}	1.2	5.746×10^{-3}	9.1209×10^{-12}	19.352×10^{-4}	0
2000 N	7.36×10^{8}	1.247	4.3×10^{-3}	6.84×10^{-12}	14.83×10^{-4}	0

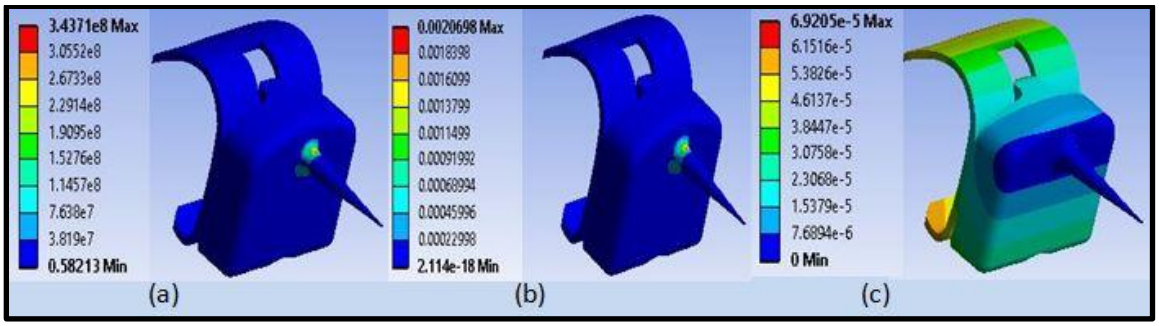

(i)

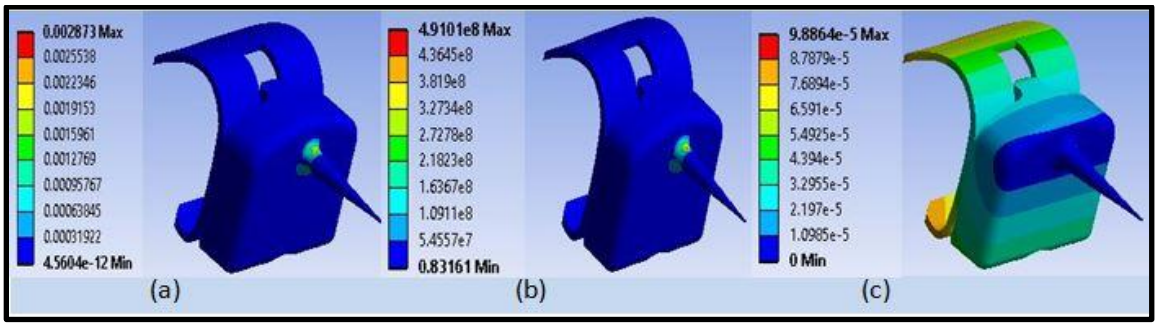

(ii)

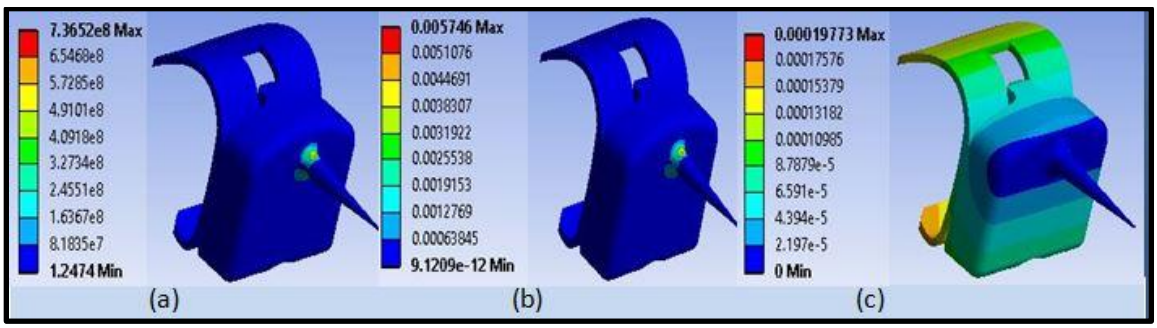

(iii)

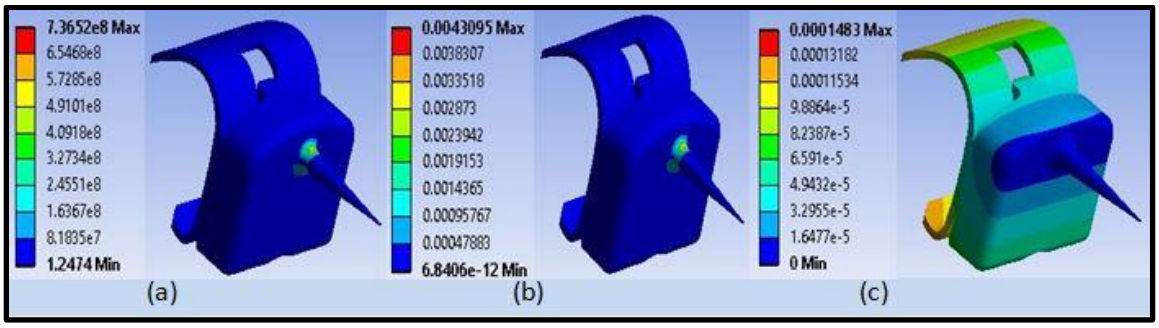

(iv)

Figure 4.1 Static analysis of the knee implant without bone using Co-Cr alloy at loading conditions of (i) 700 N, (ii) 1000 N, (iii) 1500 N and (iv) 2000 N

Figure 4.1(i-(a)) represents the stress analysis of knee implant when 700 N of force is applied. The Co-Cr alloy possesses maximum stress of 3.43×10^{8} Pa and minimum stress of 5.823×10^{1} Pa. Similarly, **Figure 4.1(i-(b))** represents the strain analysis of the knee implant. The maximum strain of 2.0689×10^{-3} and minimum strain of 2.114×10^{-18} are observed in the Co-Cr alloy. Similarly, **Figure 4.1(i-(c))** represents the total deformation analysis of knee implant. The maximum value of the total deformation of a knee implant is 6.9205×10^{-18} m.

Figure 4.1(ii-(b)) represents the stress analysis of knee implant when 1000 N of force is applied. The Co-Cr alloy possesses maximum stress of 4.9101×10^{8} Pa and minimum stress of 8.3161×10^{1} Pa. Similarly, **Figure 4.1(ii-(a))** represents the strain analysis of the knee implant without bone. The maximum strain of 2.873×10^{-3} and minimum strain of 4.5604×10^{-12} are observed in the Co-Cr alloy. Similarly, **Figure 4.1(iii-(c))** represents the total deformation analysis of knee implant. The maximum value of the total deformation a knee implant is 9.8864×10^{-5} m.

Figure 4.1(iii-(a)) represents the stress analysis of knee implant when 1500 N of force is applied. The Co-Cr alloy possesses maximum stress of 7.3652×10^{8} Pa and minimum stress of 1.2474 Pa. Similarly, **Figure 4.1(iii-(b))** represents the strain analysis of the knee implant. The maximum strain of 4.3094×10^{-3} and minimum strain of 6.8406×10^{-12} are observed in Co-Cr alloy. Similarly, **Figure 4.1(iii-(c))** represents total deformation analysis of knee implant. The maximum value of the total deformation a knee implant is 9.8864×10^{-5} m.

Figure 4.1(iv-(a)) represents the stress analysis of knee implant when 2000 N of force is applied. The Co-Cr alloy possesses maximum stress of 7.3652×10^{8} Pa and minimum stress of 1.2 Pa. Similarly, **Figure 4.1(iv-(b))** represents the strain analysis of the knee implant. The maximum strain of 5.746×10^{-3} and minimum strain of 9.1209×10^{-12} are observed in the Co-Cr alloy. Similarly, **Figure 4.1(iv-(c))** represents the total deformation analysis of knee implant. The maximum value of the total deformation a knee implant is 9.8864×10^{-5} m.

4.1.2 Static analysis of 316L SS alloy based knee implant without bone

In this case, the preprocessing and input information is same as mentioned earlier. The simulation was performed, and the maximum and minimum values of the total deformation, equivalent strain, and equivalent stress were recorded and tabulated along with their images. In the current analysis, material conditions were applied 316L SS alloy. A load of 700 N, 1000 N, 1500 N and 2000 N was used in this static analysis. **Table 4.2** represents all analysis of knee implant model without the bone. The current analysis 316L SS alloy material conditions were applied. In the solution part, we can see the maximum values of knee implant model were found. The materials along with their maximum responses are discussed in this section. Maximum equivalent stress value was recorded in the 2.51×10^{7} Pa condition. Maximum equivalent strain value was found out in the 1.489×10^{-4} m/m condition. Maximum total deformation value has been recorded in the 5.70×10^{-5} m condition.

Table 4.2 Results of static analysis knee implant without bone using 316L SS alloy

	Eq. Stress (Pa)		**Eq. Strain (m/m)**		**Total deformation (m)**	
LOAD	**Maximum Value**	**Minimum Value**	**Maximum Value**	**Minimum Value**	**Maximum Value**	**Minimum Value**
700 N	8.79×10^{6}	1.37×10^{1}	5.21×10^{-5}	1.14×10^{-10}	5.70×10^{-5}	3.4×10^{-7}
1000 N	1.25×10^{7}	1.95×10^{1}	2.87×10^{-5}	4.56×10^{-12}	9.88×10^{-5}	4.59×10^{-1}
1500 N	1.88×10^{7}	2.93×10^{1}	1.11×10^{-4}	3.04×10^{-10}	1.22×10^{-6}	7.45×10^{-1}
2000 N	2.51×10^{7}	3.94×10^{1}	1.48×10^{-4}	4.06×10^{-10}	1.62×10^{-6}	9.92×10^{-7}

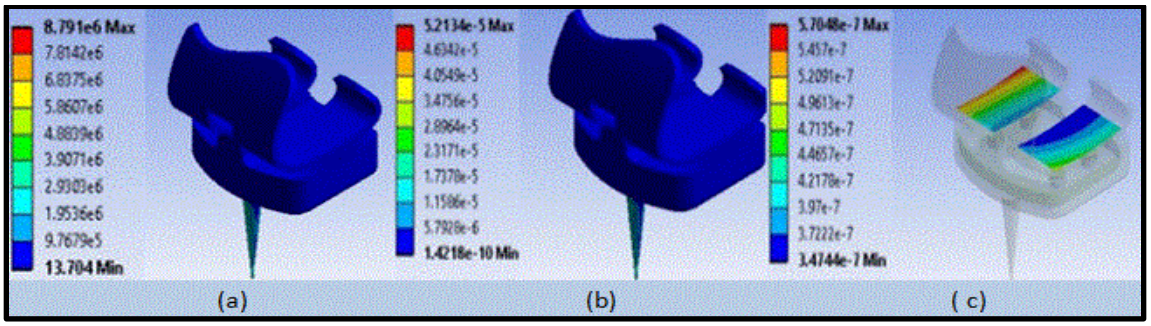

(i)

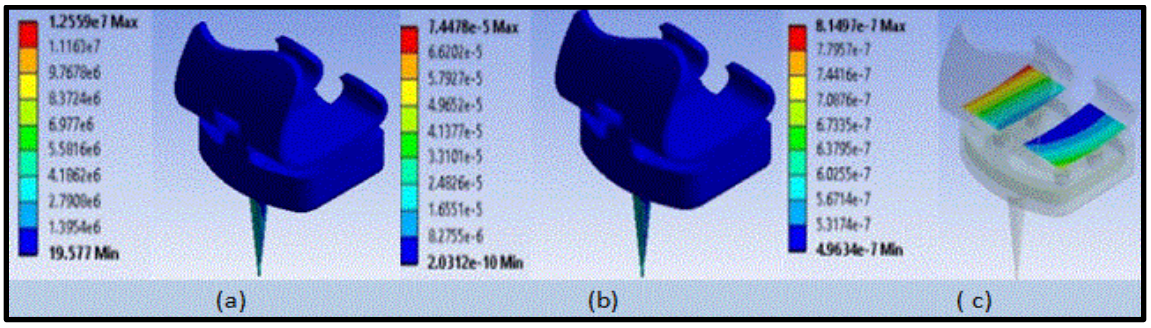

(ii)

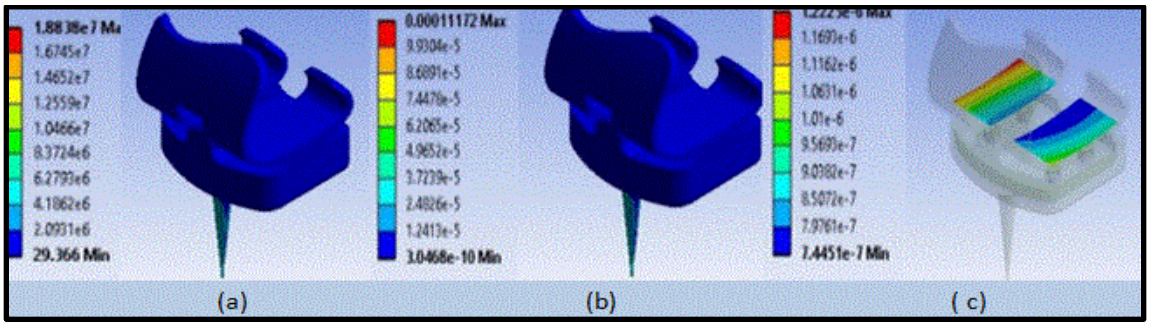

(iii)

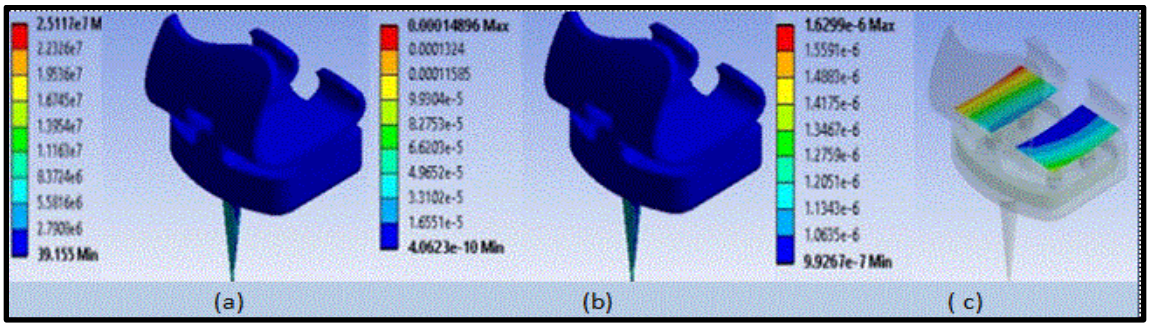

(iv)

Figure 4.2 Static analysis of the knee implant without bone using 316L SS alloy at loading conditions of (i) 700 N, (ii) 1000 N, (iii) 1500 N and (iv) 2000 N

Figure 4.2(i-(a)) represents the stress analysis of knee implant when 700 N of force is applied. The 316L SS alloy possesses maximum stress of 8.79×10^{6} Pa and minimum stress of 1.3704×10^{1} Pa. Similarly, **Figure 4.2(i-(b))** represents the strain analysis of the knee implant. The maximum strain of 5.2134×10^{-5} and minimum strain of 1.142×10^{-10} are observed in 316L SS alloy. Similarly, **Figure 4.2(i-(c))** represents total deformation analysis of the knee implant. The maximum value of total deformation knee implant without bone maximum value is 5.70×10^{-7} m.

Figure 4.2(ii-(a)) represents the stress analysis of knee implant when 1000 N of force is applied. The 316L SS alloy possesses maximum stress of 1.255×10^{7} Pa and minimum stress of 1.9577×10^{1} Pa. Similarly, **Figure 4.2(ii-(b))** represents the strain analysis of the knee implant without the bone. The maximum strain of 2.873×10^{-5} and minimum strain of 4.5604×10^{-12} are observed in the 316L SS alloy. Similarly, **Figure 4.2(ii-(c))** represents total deformation analysis of knee implant without bone. The maximum value of total deformation knee implant without bone maximum value is 9.8864×10^{-5} m.

Figure 4.2(iii-(a)) represents the stress analysis of knee implant when 1500 N of force is applied. The 316L SS alloy possesses maximum stress of 1.88×10^{7} Pa and minimum stress of 29.366 Pa. Similarly, **Figure 4.2(iii-(b))** represents the strain analysis of the knee implant without bone. The maximum strain of 1.1172×10^{-4} and minimum strain of 3.46×10^{-10} is observed in the 316L SS alloy. Similarly, **Figure 4.2(iii-(c))** represents total deformation analysis of the knee implant without bone. The maximum value of total deformation knee implant without bone is 1.225×10^{-6} m.

Figure 4.2(iv-(a)) represents the stress analysis of knee implant when 2000 N of force is applied. The 316L SS alloy possesses maximum stress of 2.511×10^{7} Pa and minimum stress of 3.9115×10^{1} Pa. Similarly, **Figure 4.2(iv-(b))** represents the strain analysis of the knee implant without the bone. The maximum strain of 1.48×10^{-4} and minimum strain of 4.0623×10^{-10} is observed in the 316L SS alloy. Similarly, **Figure 4.2(iv-(c))** represents the total deformation analysis of knee implant without the bone. The maximum value of total deformation knee implant without bone is 1.6299×10^{-6} m.

4.1.3 Static analysis of Ti6Al4V alloy based knee implant without bone

In this case, the preprocessing and input information is same as mentioned earlier. The simulation was performed, and the maximum and minimum values of the total deformation, equivalent strain, and equivalent stress were recorded and tabulated along with their images. In the current analysis, material conditions were applied Ti6Al4V alloy. A load of 700 N, 1000 N, 1500 N and 2000 N was used in this static analysis. **Table 4.3** represents all analysis of knee implant model without bone. The current analysis Ti6Al4V alloy material conditions were applied. In the solution part, we can see the maximum values of knee implant model analysis. The materials along with their maximum responses are discussed in this section. Maximum equivalent stress value was recorded in the 9.440×10^{8} Pa at the condition. Maximum equivalent strain value was recorded in the 3.858×10^{-3} m/m condition. Maximum total deformation value was recorded in the 0.00013578 m condition.

Table 4.3 Results of static analysis knee implant without bone using Ti6Al4V alloy

	Eq. Stress (Pa)		**Eq. Strain (m/m)**		**Total deformation (m)**	
LOAD	**Maximum Value**	**Minimum Value**	**Maximum Value**	**Minimum Value**	**Maximum Value**	**Minimum Value**
700 N	3.304×10^{8}	8.89×10^{-1}	3.858×10^{-3}	9.77×10^{-12}	1.357×10^{-4}	0
1000 N	4.72×10^{8}	1.27×10^{0}	5.512×10^{-3}	1.39×10^{-11}	1.939×10^{-4}	0
1500 N	7.080×10^{8}	1.90×10^{0}	8.269×10^{-3}	2.09×10^{-11}	2.909×10^{-4}	0
2000 N	9.440×10^{8}	2.54×10^{0}	1.102×10^{-2}	2.79×10^{-11}	3.879×10^{-4}	0

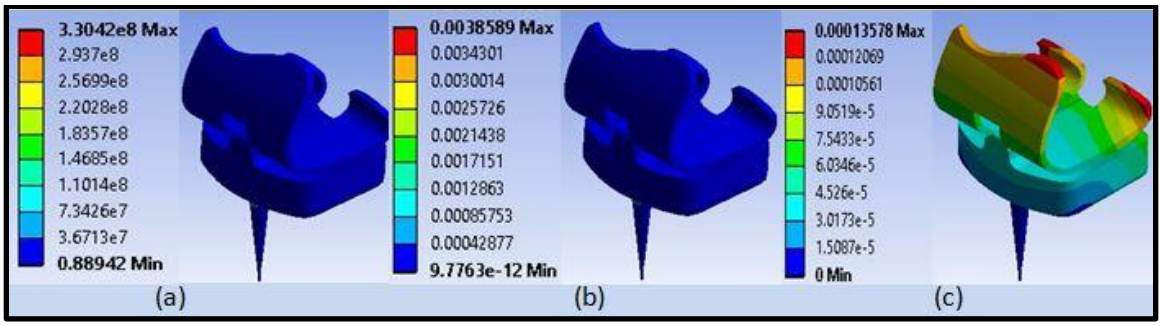

(i)

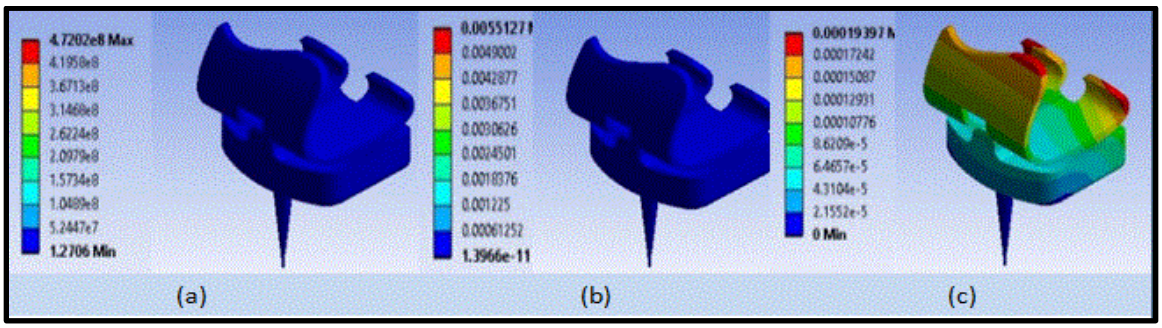

(ii)

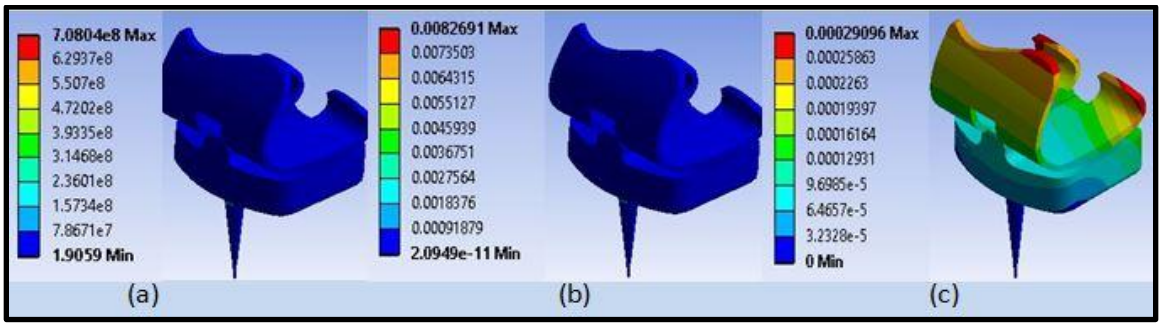

(iii)

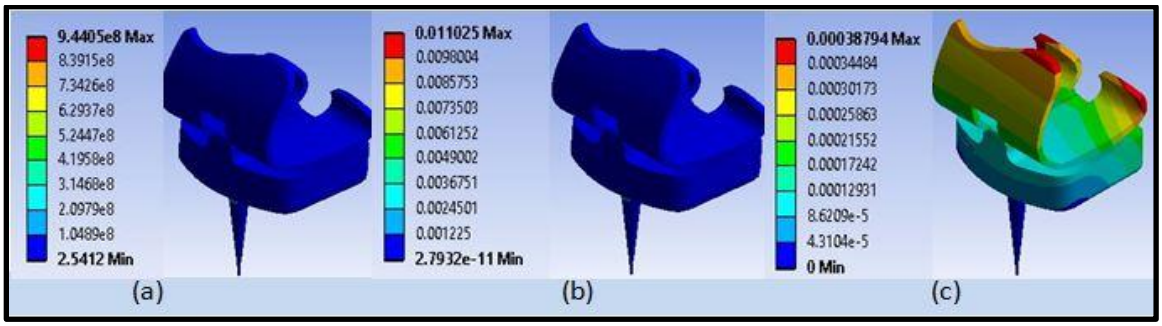

(iv)

Figure 4.3 Static analysis of the knee implant without bone using Ti6Al4V alloy at loading conditions of (i) 700 N, (ii) 1000 N, (iii) 1500 N and (iv) 2000 N

Figure 4.3(i-(a)) represents the stress analysis of knee implant when 700 N of force is applied. The Ti6Al4V alloy possesses maximum stress of 3.3042×10^{8} Pa and minimum stress of 8.8942×10^{1} Pa. Similarly, **Figure 4.3(i-(b))** represents the strain analysis of the knee implant without bone. The maximum strain of 3.8589×10^{-3} and minimum strain of 9.7763×10^{-12} is observed in the Ti6Al4V alloy. Similarly, **Figure 4.3(i-(c))** represents the total deformation analysis of the knee implant. The maximum value of total deformation knee implant is 1.3578×10^{-4} m.

Figure 4.3(ii-a)) represents the stress analysis of knee implant when 1000 N of force is applied. The Ti6Al4V alloy possesses maximum stress of 4.72×10^{8} Pa and minimum stress of 0.1279×10^{1} Pa. Similarly, **Figure 4.3(ii-(b))** represents the strain analysis of the knee implant. The maximum strain of 5.51×10^{-3} and minimum strain of 1.36×10^{-13} is observed in the Ti6Al4V alloy. Similarly, **Figure 4.3(ii-(c))** represents total deformation analysis of the knee implant. The maximum value of total deformation knee implant is 1.9×10^{-4} m.

Figure 4.3(iii-(a)) represents the stress analysis of knee implant when 1500 N of force is applied. The Ti6Al4V alloy possesses maximum stress of 7.0804×10^{8} Pa and minimum stress of 1.9059 Pa. Similarly, **Figure 4.3(iii-(b))** represents the strain analysis of the knee implant. The maximum strain of 8.2691×10^{-3} and minimum strain of 2.0949×10^{-11} is observed in the Ti6Al4V alloy. Similarly, **Figure 4.3(iii-(c))** represents total deformation analysis of the knee implant. The maximum value of total deformation knee implant is 2.9096×10^{-4} m.

Figure 4.3(iv-(a)) represents the stress analysis of knee implant when 2000 N of force is applied. The Ti6Al4V alloy possesses maximum stress of 9.4405×10^{8} Pa and minimum stress of 2.5412×10^{0} Pa. Similarly, **Figure 4.3(iv-(b))** represents the strain analysis of the knee implant. The maximum strain of 1.1025×10^{-2} and minimum strain of 2.7932×10^{-11} is observed in the Ti6Al4V alloy. Similarly, **Figure 4.3(iv-(c))** represents total deformation analysis of the knee implant without bone. The maximum value of total deformation knee implant is 3.8794×10^{-4} m.

4.1.4 Static analysis of ZrO_2 based knee implant without bone

In this case, the preprocessing and input information is same as mentioned earlier. The simulation was performed, and the maximum and minimum values of the total deformation, equivalent strain, and equivalent stress were recorded and tabulated along with their images. In the current analysis, material conditions were applied ZrO_2. A load of 700 N, 1000 N, 1500 N and 2000 N was used in this static analysis. **Table 4.4** represents all analysis of knee implant model without bone. The current analysis ZrO_2 material conditions were applied. In the solution part, we can see the maximum values of knee implant model were found. The materials along with their maximum responses are discussed in this section. Maximum equivalent stress value was recorded in the 9.8208×10^{8} Pa at the condition. Maximum equivalent strain value was founded out in the 0.00629320 condition. Maximum total deformation value was recorded in the 0.0002165 m condition.

Table 4.4 Results of static analysis knee implant without bone using ZrO_2

	Eq. Stress (Pa)		**Eq. Strain (m/m)**		**Total deformation (m)**	
LOAD	**Maximum Value**	**Minimum Value**	**Maximum Value**	**Minimum Value**	**Maximum Value**	**Minimum Value**
700 N	3.4371×10^{8}	0.58×10^{-1}	2.2026×10^{-3}	3.496×10^{-12}	7.579×10^{-5}	0
1000 N	4.9101×10^{8}	0.83×10^{-1}	3.1466×10^{-3}	4.994×10^{-12}	1.0828×10^{-4}	0
1500 N	7.3652×10^{8}	12.47×10^{-1}	4.7199×10^{-3}	7.492×10^{-12}	1.6242×10^{-4}	0
2000 N	9.8208×10^{8}	1.6632	6.2932×10^{-3}	9.989×10^{-12}	2.165×10^{-3}	0

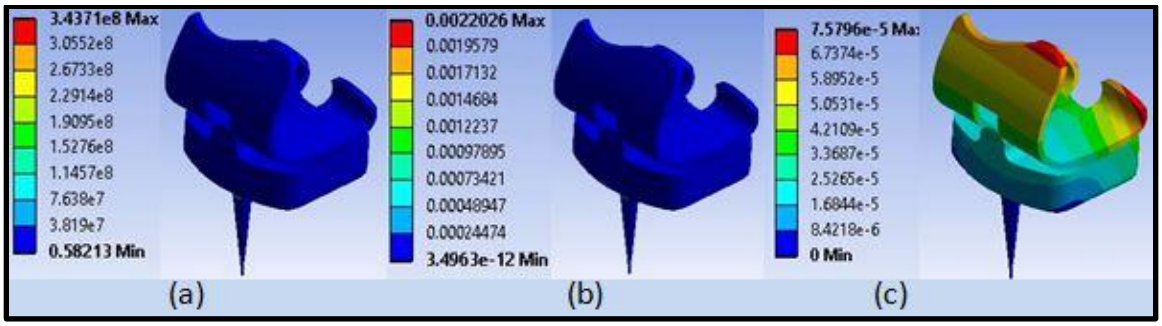

(i)

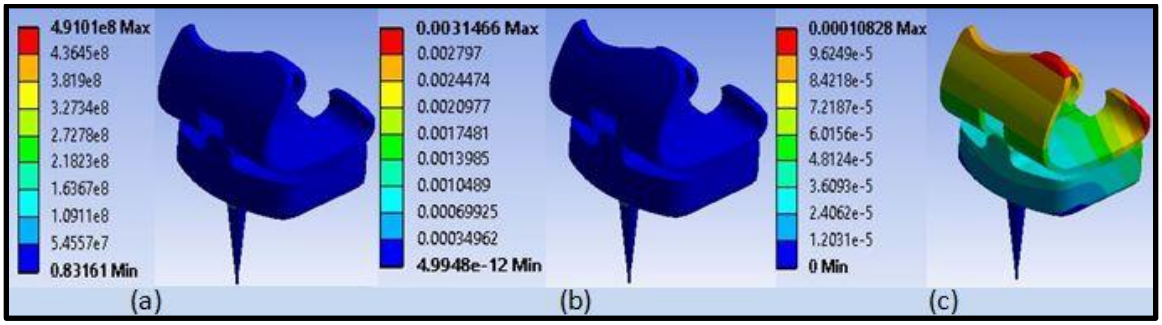

(ii)

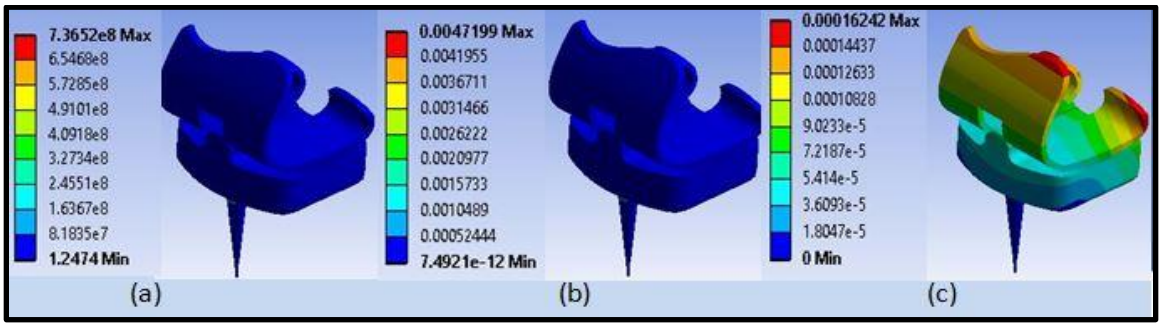

(iii)

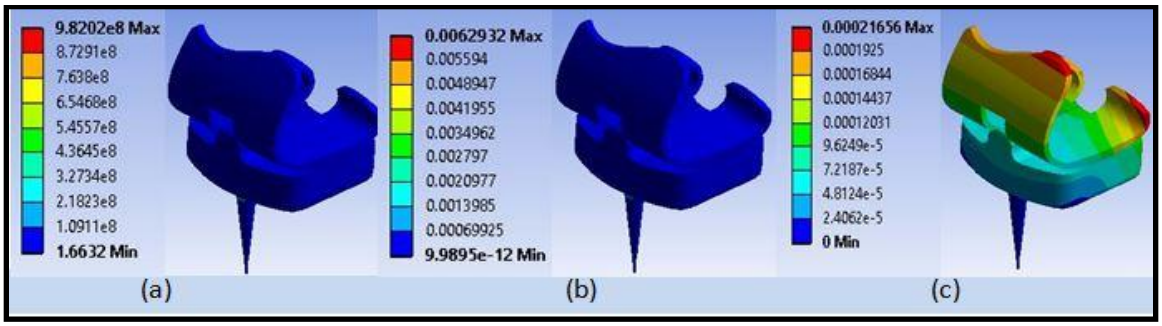

(iv)

Figure 4.4 Static analysis of the knee implant without bone using ZrO_2 at loading conditions of (i) 700 N, (ii) 1000 N, (iii) 1500 N and (iv) 2000 N

Figure 4.4(i-(a)) represents the stress analysis of knee implant when 700 N of force is applied. The ZrO_2 possesses maximum stress of 3.4371×10^8 Pa and minimum stress of 0.58213 Pa. Similarly, **Figure 4.4(i-(b))** represents the strain analysis of the knee implant without bone. The maximum strain 0.0022026 and minimum strain 3.4963×10^{-12} is observed in the ZrO_2. Similarly, **Figure 4.4(i-(c))** represents total deformation analysis of the knee implant. The maximum value of total deformation knee implant is 0.0000757 m.

Figure 4.4(ii-(a)) represents the stress analysis of knee implant when 1000 N of force is applied. The ZrO_2 possesses maximum stress of 4.9101×10^8 Pa and minimum stress of 0.83161 Pa. Similarly, **Figure 4.4(ii-(b))** represents the strain analysis of the knee implant. The maximum strain of 0.0031466 and minimum strain of 4.9948×10^{-12} is observed in the ZrO_2. Similarly, **Figure 4.4(ii-(c))** represents total deformation analysis of the knee implant. The maximum value of total deformation knee implant is 0.00007 m.

Figure 4.4(iii-(a)) represents the stress analysis of knee implant when 1500 N of force is applied. The ZrO_2 possesses maximum stress of 7.3652×10^8 Pa and minimum stress of 1.2474 Pa. Similarly, **Figure 4.4(iii-(b))** represents the strain analysis of the knee implant. The maximum strain of 0.0047199 and minimum strain of 7.4921×10^{-12} is observed in the ZrO_2. Similarly, **Figure 4.4(iii-(c))** represents the total deformation analysis of the knee implant. The maximum value of total deformation a knee implant is 0.00016242 m.

Figure 4.4(iv-(a)) represents the stress analysis of knee implant when 2000 N of force is applied. The ZrO_2 possesses maximum stress of 9.8202×10^8 Pa and minimum stress of 1.6632 Pa. Similarly, **Figure 4.4(iv-(b))** represents the strain analysis of the knee implant. The maximum strain of 0.0062932 and minimum strain of 9.9895×10^{-12} is observed in the ZrO_2. Similarly, **Figure 4.4(iv-(c))** represents the total deformation analysis of the knee implant. The maximum value of total deformation a knee implant is 0.00021656 m.

4.2 TRANSIENT ANALYSIS KNEE IMPLANT

4.2.1 Transient analysis of knee implant using time step 0.1 s

In this case, the preprocessing and input information is same as mentioned earlier. The simulation was performed, and maximum and minimum values of the total deformation, equivalent strain, and equivalent stress were recorded and tabulated along with their images. In the current analysis, three meshing conditions were applied (fine mesh, medium mesh & coarse mesh). A time step of 0.1 s was used in this transient analysis. **Table 4.5** represent maximum results of transient analysis knee implant model without bone eq. stress, eq. strain, and total deformation maximum magnitude result of individual meshing of the knee implant without bone model. Maximum eq. stress value was recorded in the 4.55×10^{8} Pa at medium meshing condition. The eq. strain value was recorded in the 2.069×10^{-3} m/m at fine meshing condition. The total deformation value was recorded in the 9.846×10^{-5} m at coarse meshing condition.

Table 4.5 Results of transient analysis of knee implant model without bone using time step 0.1 s

	Eq. Stress (Pa)		**Eq. Strain (m/m)**		**Total deformation (m)**	
Mesh	**Maximum Value**	**Minimum Value**	**Maximum Value**	**Minimum Value**	**Maximum Value**	**Minimum Value**
Coarse	3.78×10^{8}	0	20.6×10^{-4}	0.00×10^{0}	9.84×10^{-5}	0
Fine	3.70×10^{8}	5.02×10^{-7}	2.06×10^{-3}	4.2×10^{-18}	14.3×10^{-5}	0
Medium	4.5×10^{8}	3.9×10^{-6}	2.5×10^{-6}	3.8×10^{-17}	10.4×10^{-5}	0

A time step of 0.1 s was used in this transient analysis. **Figure 4.5(i-(a))** represents the stress analysis of knee implant without bone when fine meshing condition applied. The time step 0.1 s posse maximum stress of 3.7×10^{8} Pa and minimum stress of 5.02×10^{7} Pa.

Similarly, **Figure 4.5(i-(b**)) represents the strain analysis of the knee implant without bone. The maximum strain 2.069×10^{-3} and minimum strain of 4.20×10^{-18} are observed in the time step 0.1 s. Similarly, **Figure 4.5(i-(c))** represent the total deformation analysis of the knee implant without bone. The maximum value of total deformation of knee implant is 14.32×10^{-5} m.

Figure 4.5(ii-(a)) represents the stress analysis of the knee implant without bone when coarse meshing condition applied. The time step 0.1 s posse maximum eq. stress of 3.78×10^{8} Pa and minimum stress of 0 Pa. Similarly, **Figure 4.5(ii-(b))** represents the strain analysis of the knee implant without bone. The maximum strain 20.69×10^{-4} and minimum strain of 0 are observed in the time step 0.1 s. Similarly, **Figure 4.5(ii-(c))** represents the total deformation analysis of a knee implant without bone. The maximum value of total deformation knee implant is 9.846×10^{-5} m.

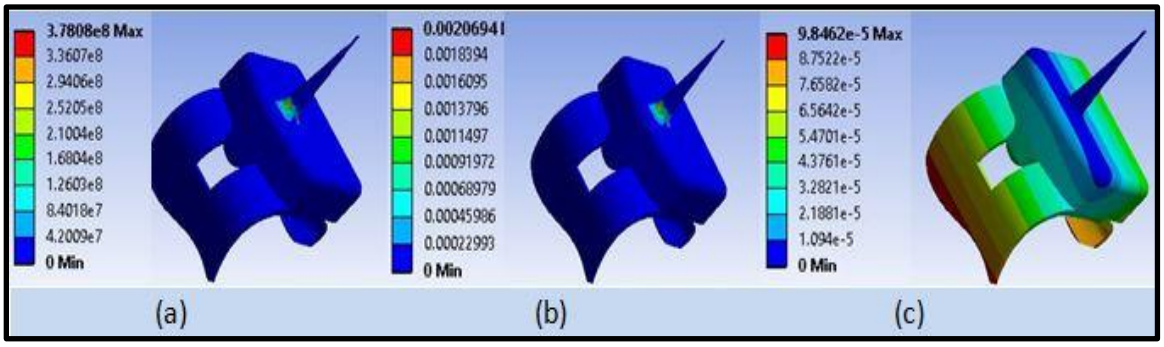

(i)

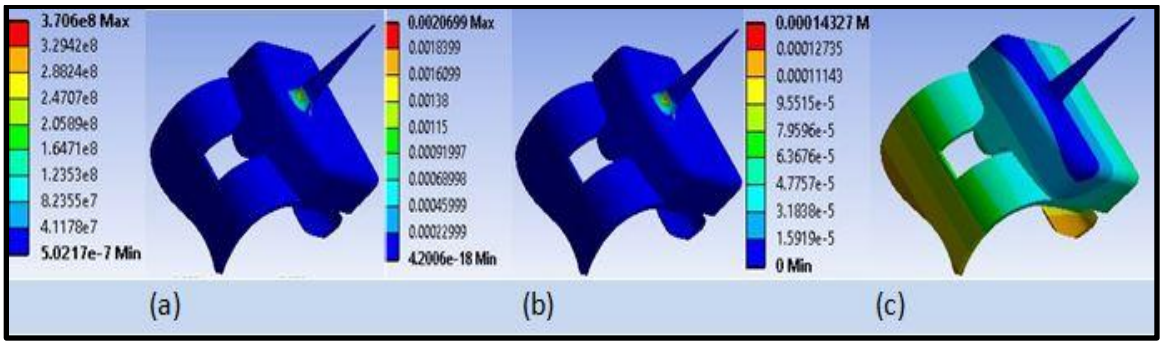

(ii)

Figure 4.5 Transient analysis of the knee implant without bone using 0.1 s time step (i) coarse mesh, (ii) fine mesh represents

4.2.2 Transient analysis of knee implant using time step 0.01 s

In this case, the preprocessing and input information is same as mentioned earlier. The simulation was performed, and the maximum and minimum values of the total deformation, equivalent strain, and equivalent stress were recorded and tabulated along with their images. In the current analysis, three meshing conditions were applied (fine mesh, medium mesh and coarse mesh). A time step of 0.01 s was used in this transient analysis. **Table 4.6** represents the eq. stress, eq. strain, and total deformation maximum magnitude result of individual meshing condition after the analytical work was performed. Maximum eq. stress value was recorded in the 3.786×10^{8} Pa at coarse meshing condition. Maximum eq. strain value was recorded in the 0.0020693 at coarse mesh condition. Maximum total deformation value was recorded in the 2.069×10^{-3} m at coarse mesh condition.

Table 4.6 Results of transient analysis knee implant model without bone using time step 0.01 s

	Eq. Stress (Pa)		**Eq. Strain (m/m)**		**Total deformation (m)**	
MESH	**Maximum Value**	**Minimum Value**	**Maximum Value**	**Minimum Value**	**Maximum Value**	**Minimum Value**
Coarse	3.78×10^{8}	0	0.0020	0	1.4×10^{-4}	0
Fine	3.70×10^{8}	0	20.6×10^{-4}	4.2×10^{-18}	9.8×10^{-5}	0
Medium	2.59×10^{8}	2.32×10^{-6}	14.1×10^{-4}	2.0×10^{-17}	8.5×10^{-5}	0

A time step of 0.01 s was used in this transient analysis. **Figure 4.6(i-(a))** represents the stress analysis of knee implant without bone when fine meshing condition applied. The time step 0.01 s posse maximum stress 3.70×10^{8} Pa and minimum stress 0 Pa. Similarly, **Figure 4.6(i-(b))** represents the strain analysis of the knee implant without bone. The

maximum strain 20.69×10^{-4} and minimum strain 0 are observed in the time step 0.01 s. Similarly, **Figure 4.6(i-(c))** represent the total deformation analysis of the knee implant without bone. The total deformation of knee implant without bone maximum value is 9.845×10^{-5} m.

A time step of 0.01 s was used in this transient analysis. **Figure 4.6(ii-(a))** represents the stress analysis of knee implant without bone when coarse meshing condition applied. The time step 0.01 s posse maximum stress of 3.786×10^{8} Pa and minimum stress of 0 Pa. Similarly, **Figure 4.6(ii-(b**)) represents the strain analysis of the knee implant without bone. The maximum strain 0.0020693 and minimum strain of 0 is observed in the time step 0.01 s. Similarly, **Figure 4.6(ii-(c))** represents the total deformation analysis of the knee implant. The total deformation of knee implant maximum value is 1.4×10^{-4} m.

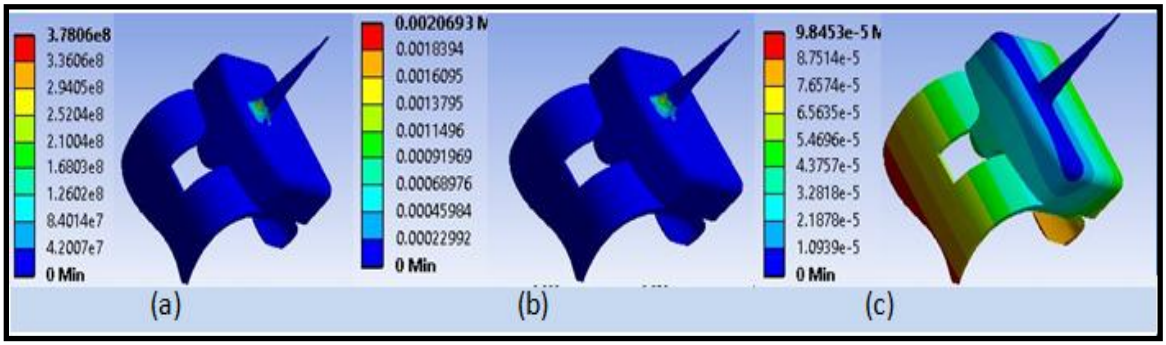

(i)

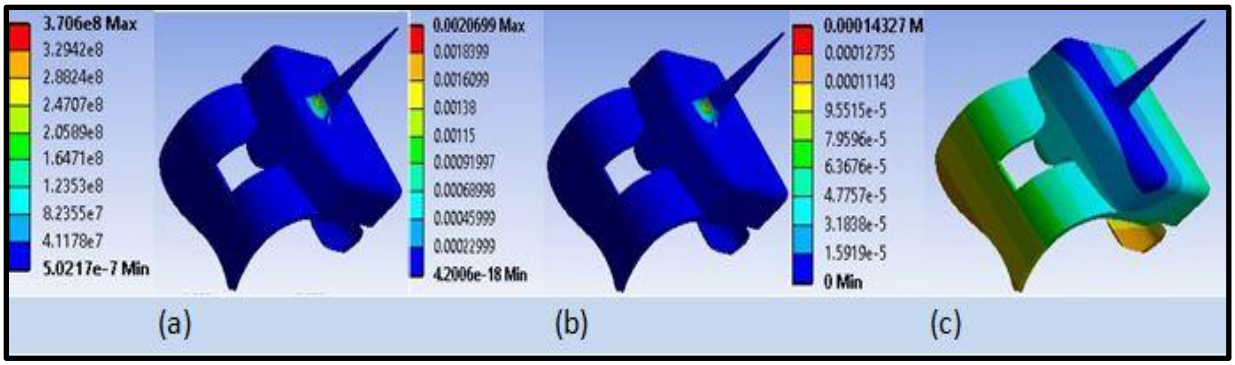

(ii)

Figure 4.6 Transient analysis of the knee implant without bone using 0.01 s time step (i) coarse mesh and (ii) fine mesh

4.2.3 Transient analysis of knee implant using time Step 0.001 s.

In this case, the preprocessing and input information is same as mentioned earlier. The simulation was performed, and the maximum and minimum values of the total deformation, equivalent strain, and equivalent stress were recorded and tabulated along with their images. In the current analysis, three meshing conditions were applied (fine mesh, medium mesh & coarse mesh). A time step of 0.001 s was used in this transient analysis. **Table 4.7** represents the eq. stress, eq. strain, and total deformation maximum magnitude results of individual mesh condition after the analytical work was performed. Maximum eq. stress value was recorded in the 4.55×10^{8} Pa at medium mesh condition. Maximum eq. Strain value was recorded in the 2.06×10^{-3} at fine mesh condition. Maximum total deformation value was recorded in the 2.069×10^{-3} m at coarse mesh condition.

Table 4.7 Results of transient analysis knee implant model without bone using time step 0.001 s

	Eq. Stress (Pa)		**Eq. Strain (m/m)**		**Total deformation (m)**	
MESH	**Maximum Value**	**Minimum Value**	**Maximum Value**	**Minimum Value**	**Maximum Value**	**Minimum Value**
Coarse	3.780×10^{8}	0	2.060×10^{-3}	0	14×10^{-5}	0
Fine	3.70×10^{8}	0.103×10^{6}	2.060×10^{-3}	2.11×10^{-18}	14.320×10^{-5}	0
Medium	4.550×10^{8}	3.90×10^{6}	2.500×10^{-6}	3.800×10^{-17}	10.430×10^{-5}	0

A time step of 0.001 s was used in this transient analysis. **Figure 4.7(i-(a))** represents the stress analysis of knee implant without bone when fine meshing condition applied. The time step 0.001 s posse maximum stress of 370.6×10^{6} Pa and minimum stress of 0.103×10^{-6} Pa. Similarly, **Figure 4.7(i-(b))** represents the strain analysis of the knee

implant without bone. The maximum strain 2.06×10^{-3} and minimum strain 2.11×10^{-18} of is observed in the time step 0.001 s. Similarly, **Figure 4.7(i-(c))** represent the total deformation analysis of the knee implant without bone. The total deformation of knee implant without bone maximum value is 14.32×10^{-5} m.

A time step of 0.001 s was used in this transient analysis. **Figure 4.7(ii-(a))** represents the stress analysis of knee implant without bone when fine meshing condition applied. The time step 0.001 s posse maximum stress value of 3.7×10^{8} Pa and minimum stress of value 0 Pa. Similarly, **Figure 4.7(ii-(b))** represents the strain analysis of the knee implant without bone. The maximum strain 2.069×10^{-3} and minimum strain of 0 are observed in the time step 0.001 s. Similarly, **Figure 4.7(ii-(c))** represents the total deformation analysis knee implant without bone. The total deformation of knee implant without bone maximum value is 14×10^{-5} m.

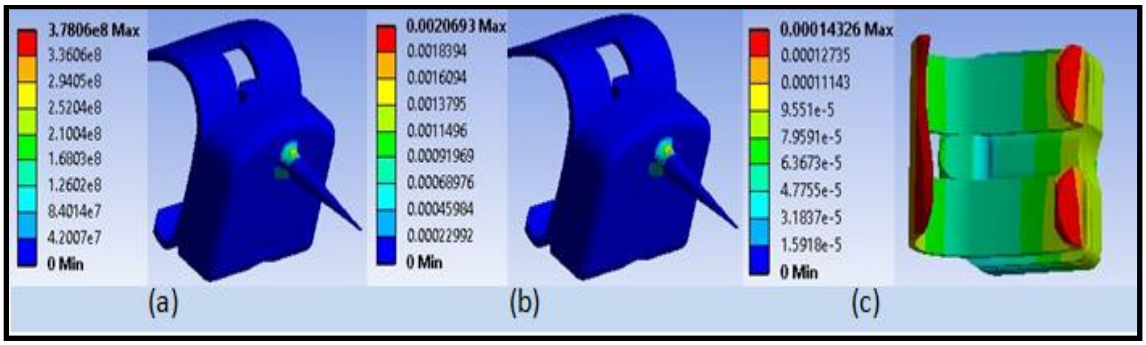

(i)

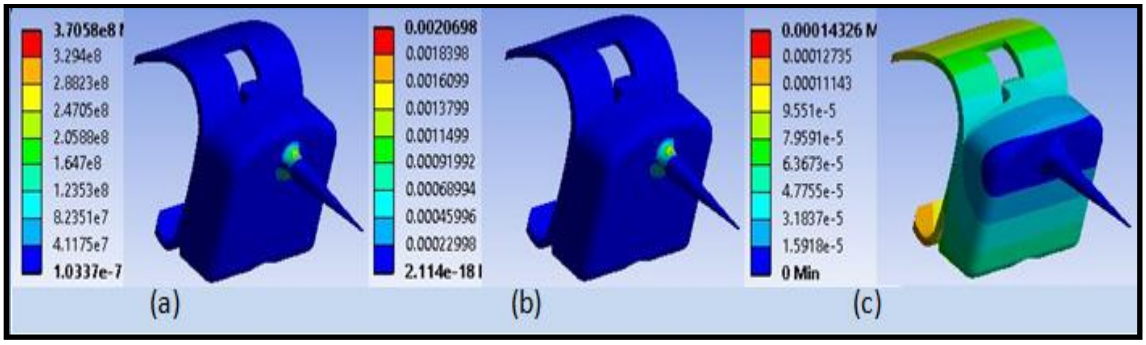

(ii)

Figure 4.7 Transient analysis of the knee implant without bone using 0.001 s time step (i) coarse mesh and (ii) fine mesh.

4.3 STATIC ANALYSIS KNEE IMPLANT WITH BONE

4.3.1 Static analysis of Co-Cr alloy based knee implant with bone

In this case, the preprocessing and input information is same as mentioned earlier. The simulation was performed, and the maximum and minimum values of the total deformation, equivalent strain, and equivalent stress were recorded and tabulated along with their images. In the current analysis, material conditions were applied Co-Cr alloy. A load of 700 N, 1000 N, 1500 N and 2000 N was used in this static analysis. **Table 4.8** represents all analysis of knee implant model with bone. The current analysis Co-Cr alloy material conditions were applied. In the solution part, we can see the maximum values of knee implant model were found. The materials along with their maximum responses are discussed in this section. Maximum eq. stress value was recorded in the 19.613×10^{8} Pa condition. Maximum eq. strain value was recorded in the 1478.1 condition. Maximum total deformation value was recorded in the 27.136 m condition.

Table 4.8 Results of static analysis knee implant with bone using Co-Cr alloy

	Eq. Stress (Pa)		**Eq. Strain (m/m)**		**Total deformation (m)**	
LOAD	**Maximum Value**	**Minimum Value**	**Maximum Value**	**Minimum Value**	**Maximum Value**	**Minimum Value**
700 N	6.8×10^{8}	1.04×10^{3}	5.17×10^{2}	9.99×10^{-6}	0.94×10^{1}	0
1000 N	9.80×10^{8}	1.49×10^{3}	7.93×10^{2}	0.142×10^{-6}	1.35×10^{1}	0
1500 N	14.7×10^{8}	2.23×10^{3}	1.10×10^{2}	0.21×10^{-6}	2.03×10^{1}	0
2000 N	19.6×10^{8}	2.98×10^{3}	1.47×10^{2}	0.28×10^{-6}	2.71×10^{1}	0

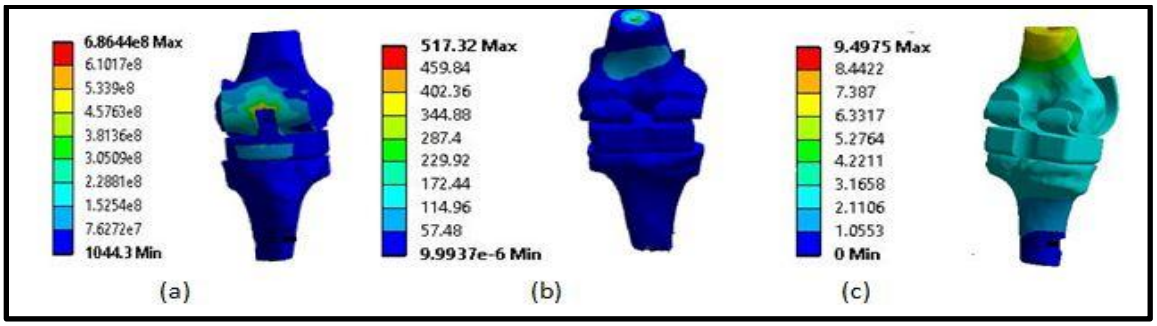

(i)

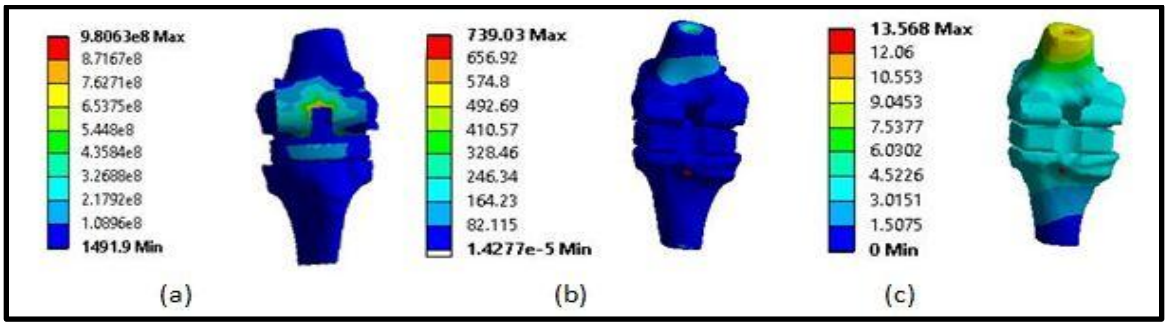

(ii)

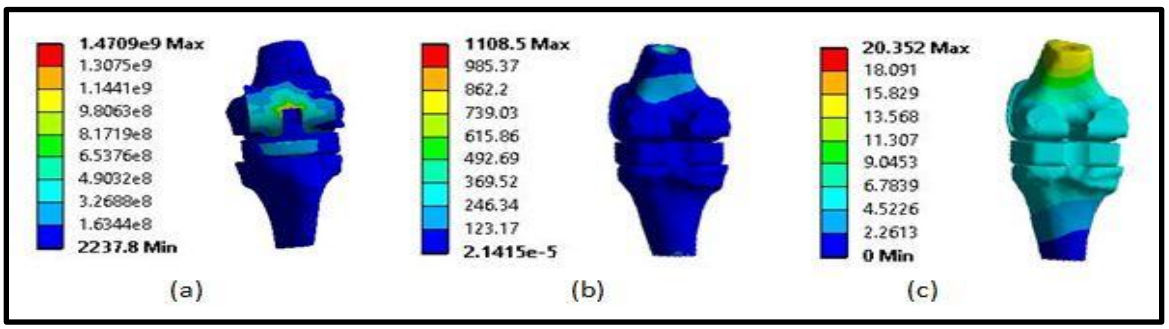

(iii)

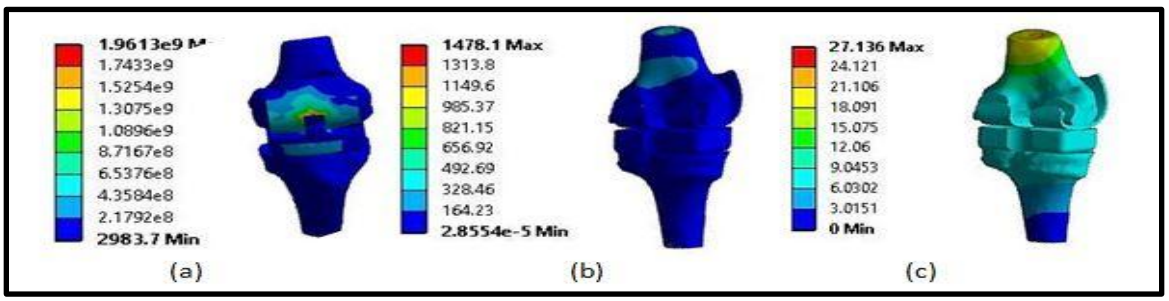

(iv)

Figure 4.8 Static analysis of the knee implant with bone using Co-Cr alloy at loading conditions of (i) 700 N, (ii) 1000 N, (iii) 1500 N and (iv) 2000 N

Figure 4.8(i-(a)) **re**presents the stress analysis results of knee implant with bone when 700 N of force is applied. The Co-Cr alloys possess maximum stress of 6.864×10^{8} Pa and minimum stress of 1.044×10^{3} Pa. Similarly, **Figure 4.8(i-(b))** the strain analysis of the knee implant with bone. The maximum strain of 5.172×10^{2} and minimum strain of 9.9937×10^{-6} is observed in the Co-Cr alloy. Similarly, **Figure 4.8(i-(c))** total deformation analysis of the knee implant with bone. The total deformation of knee implant with bone maximum value is 0.94975×10^{1} m.

Figure 4.8(ii-(a)) the stress analysis of knee implant with bone when 1000 N of force is applied. The Co-Cr alloy possesses maximum stress of 9.8063×10^{8} Pa and minimum stress of 1.4919×10^{3} Pa. Similarly, **Figure 4.8(ii-(b))** the strain analysis of the knee implant with bone. The maximum strain of 7.9303×10^{2} and minimum strain of 0.1427×10^{-6} is observed in the Co-Cr alloy. Similarly, **Figure 4.8(ii-(c))** total deformation analysis of the knee implant with bone. The total deformation of knee implant with bone maximum value is 1.3568×10^{01} m.

Figure 4.8(iii-(a)) represents the stress analysis of knee implant with bone when 1500 N of force is applied. The Co-Cr alloy possesses maximum stress of 14.709×10^{8} Pa and minimum stress of 2.2378×10^{3} Pa. Similarly, **Figure 4.8(iii-(b))** the strain analysis of the knee implant with bone. The maximum strain of 1.1085×10^{3} and minimum strain of 0.2141×10^{-6} is observed in the Co-Cr alloy. Similarly, **Figure 4.8(iii-(c))** represents the total deformation analysis of the knee implant with bone. The total deformation of knee implant with bone maximum value is 2.0352×10^{1} m.

Figure 4.8(iv-(a)) represents the stress analysis of knee implant with bone when 2000 N of force is applied. The Co-Cr alloy possesses maximum stress of 19.613×10^{8} Pa and minimum stress of 2.9837×10^{3} Pa. Similarly, **Figure 4.8(iv-(b))** represents the strain analysis of the knee implant with bone. The maximum strain of 1478.1 and minimum strain of 0.2855×10^{-6} are observed in the Co-Cr alloy. Similarly, **Figure 4.8(iv-(c))** represents total deformation analysis of the knee implant with bone. The total deformation of knee implant with bone maximum value is 27.136 m.

4.3.2 Static analysis of 316L SS alloy based knee implant with bone

In this case, the preprocessing and input information is same as mentioned earlier. The simulation was performed, and maximum and minimum values of the total deformation, equivalent strain, and equivalent stress were recorded and tabulated along with their images. In the current analysis, four material conditions were applied 316L SS alloy. A load of 700 N, 1000 N, 1500 N and 2000 N was used in this static analysis. **Table 4.9** represents all analysis of knee implant model with bone. The current analysis 316L SS alloy material conditions were applied. In the solution part, we can see the maximum values of knee implant model were found. The materials along with their maximum responses are discussed in this section. Maximum equivalent stress value was recorded in the 27.622×10^{8} Pa condition. Maximum equivalent strain value was recorded in the 1478.1 condition. Maximum total deformation value was recorded in the 27.11 m condition.

Table 4.9 Results of static analysis knee implant with bone using 316L SS alloy

	Eq. Stress (Pa)		**Eq. Strain (m/m)**		**Total deformation (m)**	
LOAD	**Maximum Value**	**Minimum Value**	**Maximum Value**	**Minimum Value**	**Maximum Value**	**Minimum Value**
700 N	9.62×10^{8}	1044.7	517.33	5.65×10^{-6}	9.48	0
1000 N	13.7×10^{8}	1492.5	739.06	8.07×10^{-6}	13.55	0
1500 N	20.0×10^{8}	2238.7	1108.52	0.12×10^{-6}	20.33	0
2000 N	27×10^{8}	2985	1478.13	0.16×10^{-6}	27.11	0

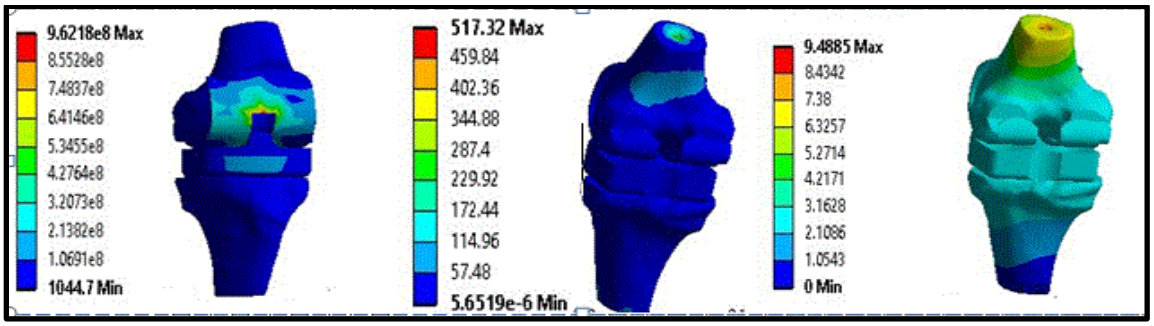

(i)

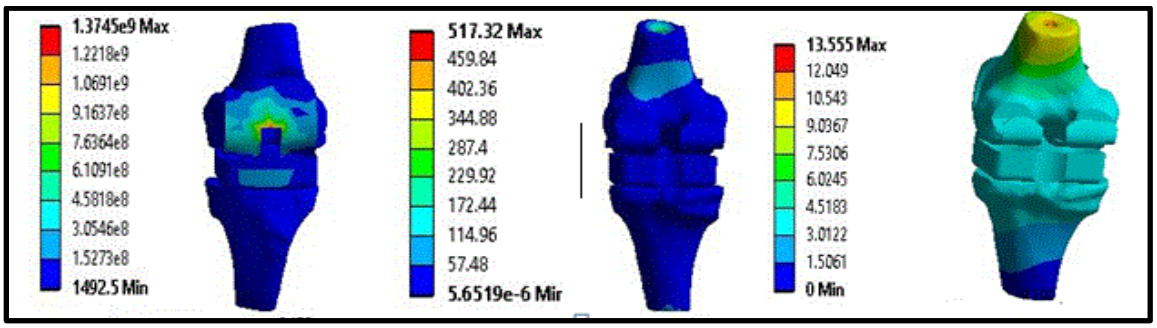

(ii)

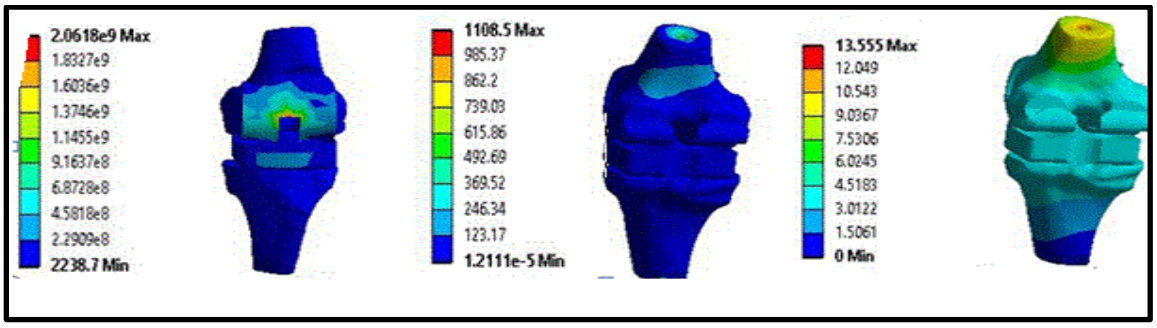

(iii)

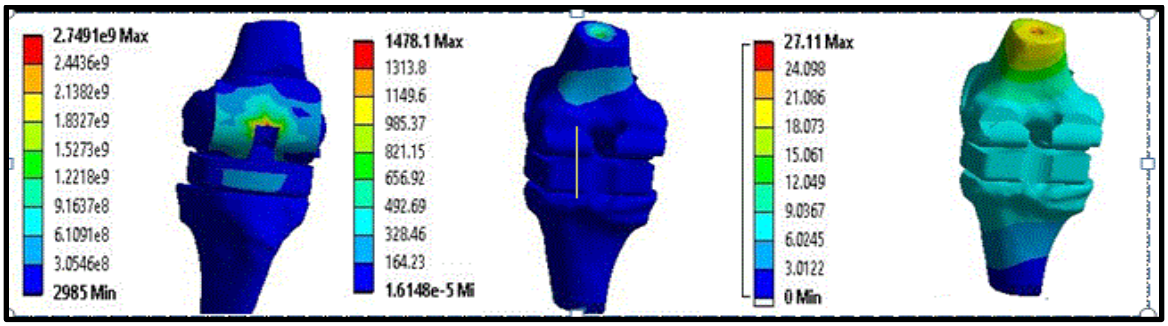

(iv)

Figure 4.9 Static analysis of the knee implant with bone using 316L SS alloy at loading conditions of (i) 700 N, (ii) 1000 N, (iii) 1500 N, (iv) 2000 N

Figure 4.9(i-(a)) the stress analysis of knee implant with bone when 700 N of force is applied. The 316L SS alloy possesses maximum stress of 9.621×10^{8} Pa and minimum stress of 1044.7 Pa. Similarly, **Figure 4.9(i-(b))** the strain analysis of the knee implant with bone. The maximum strain of 517.33 and minimum strain of 5.65×10^{-6} is observed in the 316L SS alloy. Similarly, **Figure 4.9(i-(c))** represents the total deformation analysis of the knee implant with bone. The total deformation of knee implant with bone maximum value is 9.488 m.

Figure 4.9(ii-(a)) the stress analysis of knee implant with bone when 1000 N of force is applied. The 316L SS alloy possesses maximum stress of 13.745×10^{8} Pa and minimum stress of 1492.5 Pa. Similarly, **Figure 4.9(ii-(b))** the strain analysis of the knee implant with bone. The maximum strain of 739.06 and minimum strain of 8.074×10^{-6} is observed in the 316L SS alloy. Similarly, **Figure 4.9(ii-(c))** represents the total deformation analysis of the knee implant with bone. The total deformation of knee implant with bone maximum value is 13.555 m.

Figure 4.9(iii-(a)) the stress analysis of knee implant with bone when 1500 N of force is applied. The 316L SS alloy possesses maximum stress of 20.061×10^{8} Pa and minimum stress of 2238.7 Pa. Similarly, **Figure 4.9(iii-(b))** the strain analysis of the knee implant with bone. The maximum strain of 1108.52 and minimum strain of 0.121×10^{-6} is observed in the 316L SS alloy. Similarly, **Figure 4.9(iii-(c))** represents the total deformation analysis of the knee implant with bone. The total deformation of knee implant with bone maximum value is 20.33 m.

Figure 4.9(iv-(a)) the stress analysis of knee implant with bone when 2000 N of force is applied. The 316L SS alloy possesses maximum stress of 27.49×10^{8} Pa and minimum stress of 2985 Pa. Similarly, **Figure 4.9(iv-(b))** the strain analysis of the knee implant with bone. The maximum strain of 1478.13 and minimum strain of 0.161×10^{-6} is observed in the 316L SS alloy. Similarly, **Figure 4.9(iv-(c))** represents the total deformation analysis of the knee implant with bone. The total deformation of knee implant with bone maximum value is 27.11 m.

4.3.3 Static analysis of Ti6Al4V alloy based knee implant with bone

In this case, the preprocessing and input information is same as mentioned earlier. The simulation was performed, and the maximum and minimum values of the total deformation, equivalent strain, and equivalent stress were recorded and tabulated along with their images. In the current analysis, Ti6Al4V alloy loading conditions were applied alloy. A load of 700 N, 1000 N, 1500 N and 2000 N was used in this static analysis. **Table 4.10** represents all analysis of knee implant model with bone. The current analysis Ti6Al4V alloy material conditions were applied. In the solution part, we can see the maximum values of knee implant mode were found. The materials along with their maximum responses are discussed in this section. Maximum equivalent stress value was recorded in the 29.622×10^{8} Pa condition. Maximum equivalent strain value was recorded in the 1478.1 condition. Maximum total deformation value was recorded in the 27.103 m condition.

Table 4.10 Results of static analysis knee implant with bone using Ti6Al4V alloy

	Eq. Stress (Pa)		**Eq. Strain (m/m)**		**Total deformation (m)**	
Load	**Maximum Value**	**Minimum Value**	**Maximum Value**	**Minimum Value**	**Maximum Value**	**Minimum Value**
700 N	10.36×10^{8}	1045.1	517.32	4.959×10^{-6}	9.4861	0
1000 N	14.81×10^{8}	1492.9	739.03	7.085×10^{-6}	13.552	0
1500 N	22.21×10^{8}	2239.4	1108.5	1.062×10^{-6}	20.327	0
2000 N	29.62×10^{8}	2985.8	1478.1	0.141×10^{-6}	27.103	0

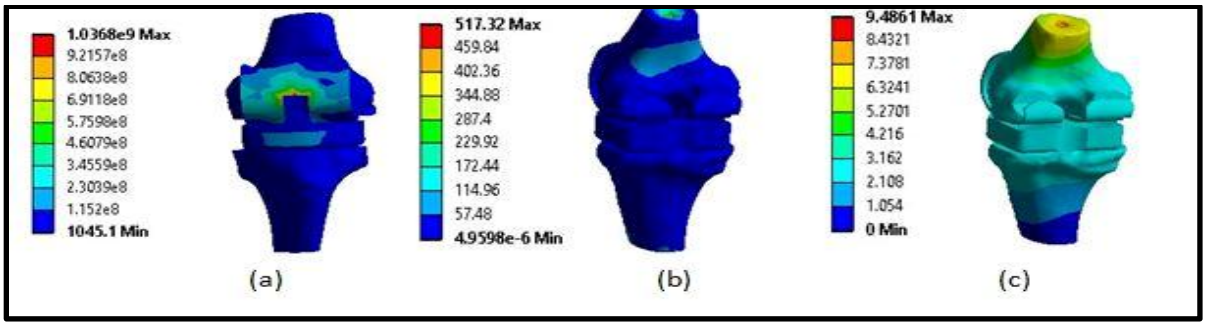

(i)

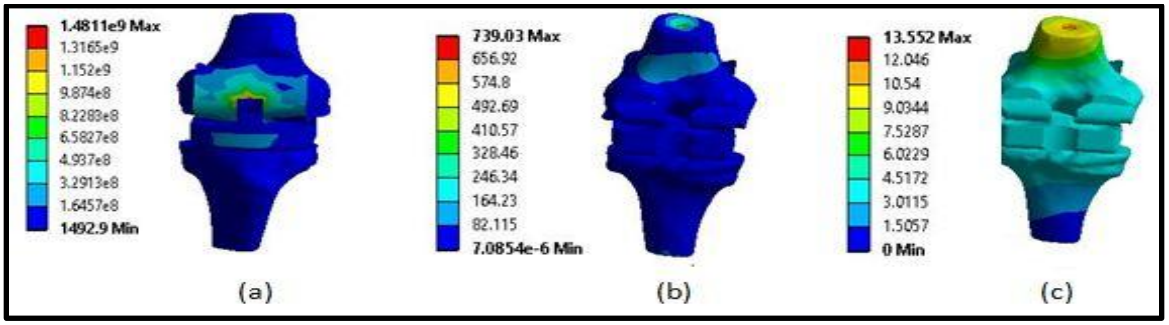

(ii)

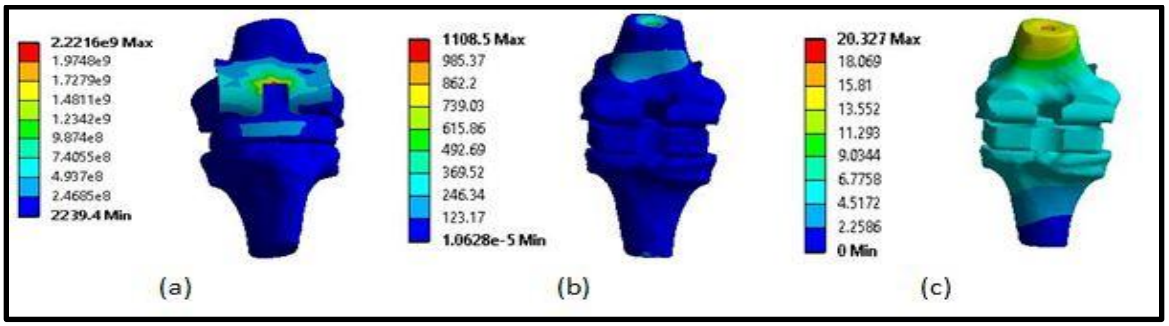

(iii)

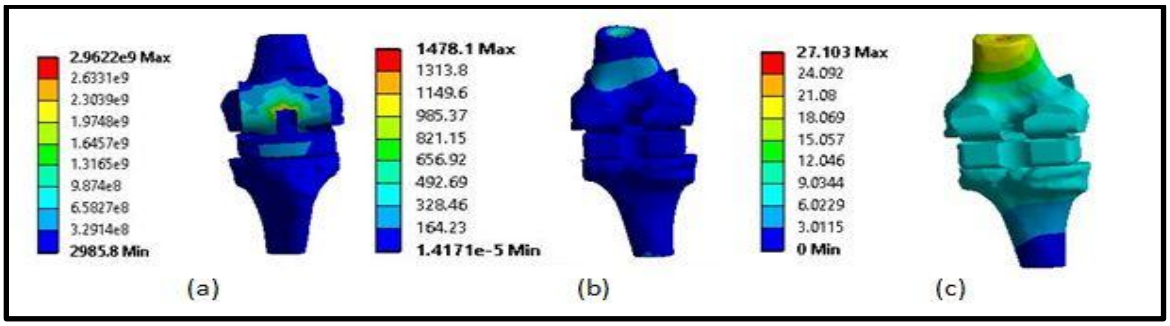

(iv)

Figure 4.10 Static analysis of the knee implant with bone using Ti6Al4V alloy at loading conditions of (i) 700 N, (ii) 1000 N, (iii) 1500 N and (iv) 2000 N

Figure 4.10(i-(a)) the stress analysis of knee implant with bone when 700 N of force is applied. The Ti6Al4V alloy maximum posse stress of 10.36×10^{8} Pa and minimum stress of 1045.1 Pa. Similarly, **Figure 4.10(i-(b))** the strain analysis of the knee implant with bone. The maximum strain of 517.32 and minimum strain of 4.959×10^{-6} is observed in the Ti6Al4V alloy. Similarly, **Figure 4.10(i-(c))** represents the total deformation analysis of the knee implant with bone. The total deformation of knee implant with bone maximum value is 9.4861 m.

Figure 4.10(ii-(a)) the stress analysis of knee implant with bone when 1000 N of force is applied. The Ti6Al4V alloy possesses maximum stress of 14.811×10^{8} Pa and minimum stress of 1492.9 Pa. Similarly, **Figure 4.10(ii-(b))** the strain analysis of the knee implant with bone. The maximum strain of 739.03 and minimum strain of 7.0854×10^{-6} is observed in the Ti6Al4V alloy. Similarly, **Figure 4.10(ii-(c))** represents total deformation analysis of the knee implant with bone. The total deformation of knee implant with bone maximum value is 13.552 m.

Figure 4.10(iii-(a)) the stress analysis of knee implant with bone when 1500 N of force is applied. The Ti6Al4V alloy possesses maximum stress of 22.216×10^{8} Pa and minimum stress of 2239.4 Pa. Similarly, **Figure 4.10(iii-(b))** the strain analysis of the knee implant with bone. The maximum strain of 1108.5 and minimum strain of 1.0628×10^{-6} is observed in the Ti6Al4V alloy. Similarly, **Figure 4.10(iii-(c))** represents the total deformation analysis of the knee implant with bone. The total deformation of knee implant with bone maximum value is 20.327 m.

Figure 4.10(iv-(a)) the stress analysis of knee implant with bone when 2000 N of force is applied. The Ti6Al4V alloy possesses maximum stress of 29.622×10^{8} Pa and minimum stress of 2985.8 Pa. Similarly, **Figure 4.10(iv-(b))** the strain analysis of the knee implant with bone. The maximum strain of 1478.1 and minimum strain of 0.1417×10^{-6} is observed in the Ti6Al4V alloy. Similarly, **Figure 4.10(iv-(c))** represents the total deformation analysis of the knee implant with bone. The total deformation of knee implant with bone maximum value is 27.103 m

4.3.4 Static analysis of ZrO_2 based knee implant with bone

In this case, the preprocessing and input information is same as mentioned earlier. The simulation was performed, and the maximum and minimum values of the total deformation, equivalent strain, and equivalent stress were recorded and tabulated along with their images. In the current analysis, four loading conditions were applied ZrO_2. A load of 700 N, 1000 N, 1500 N and 2000 N was used in this static analysis. **Table 4.11** represents all analysis of knee implant model with bone. The current analysis ZrO_2 material conditions were applied. In the solution part, we can see the maximum values of knee implant model were found. The materials along with their maximum responses are discussed in this section. Maximum equivalent stress value was recorded in the 28.562×10^8 Pa condition. Maximum equivalent strain value was recorded in the 1478.1 m/m condition. Maximum total deformation value was recorded in the 27.107 m condition.

TABLE 4.11 Results of static analysis knee implant with bone using ZrO_2

	Eq. Stress (Pa)		**Eq. Strain (m/m)**		**Total deformation (m)**	
Load	**Maximum Value**	**Minimum Value**	**Maximum Value**	**Minimum Value**	**Maximum Value**	**Minimum Value**
700 N	9.99×10^8	1044.8	517.32	5.28×10^{-6}	9.875	0
1000 N	14.2×10^8	1492.7	739.03	7.55×10^{-6}	13.554	0
1500 N	21.4×10^8	2239	1108.5	11.3×10^{-6}	20.33	0
2000 N	28.5×10^8	2985.3	1478.1	15.1×10^{-6}	27.107	0

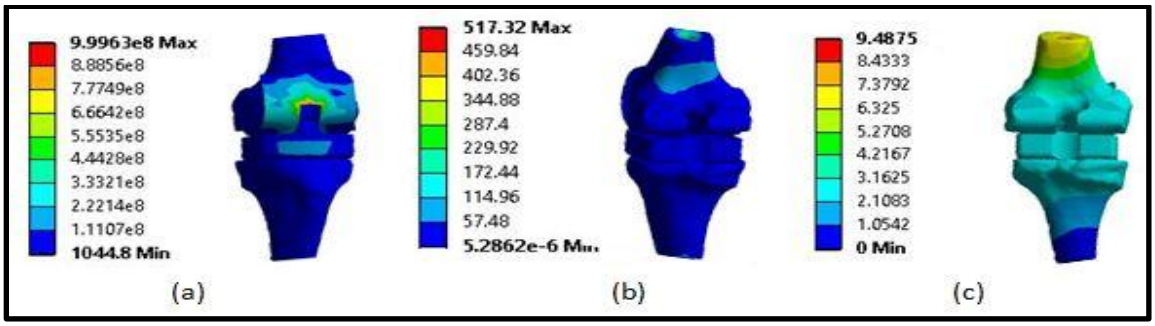

(i)

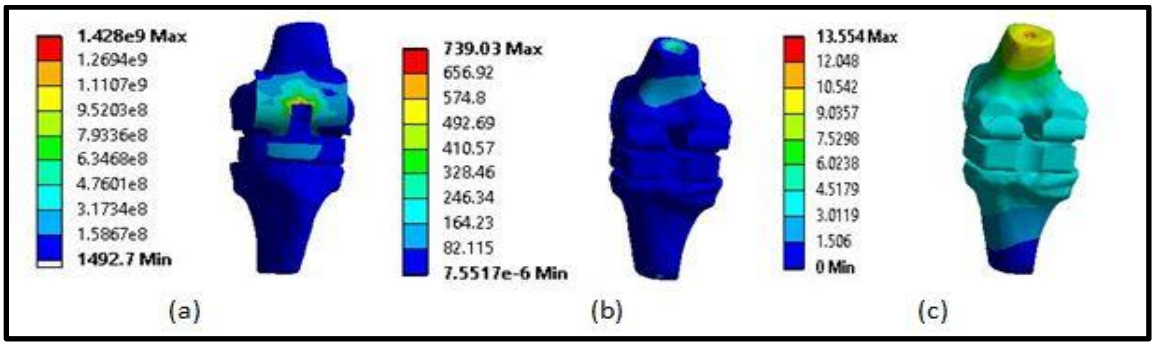

(ii)

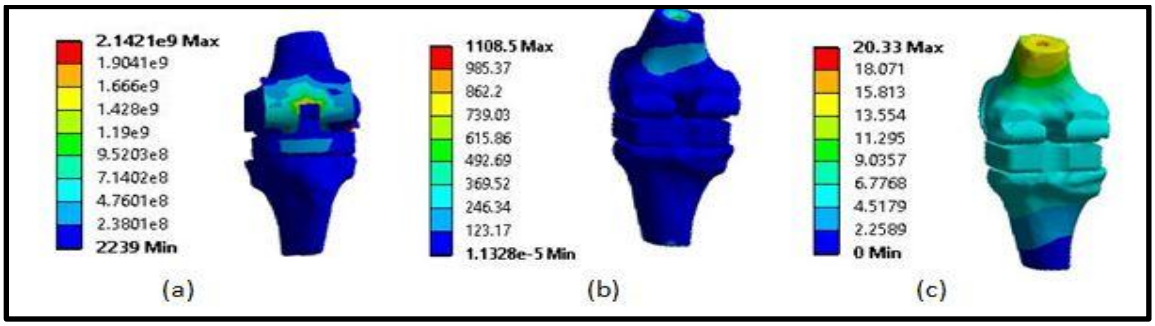

(iii)

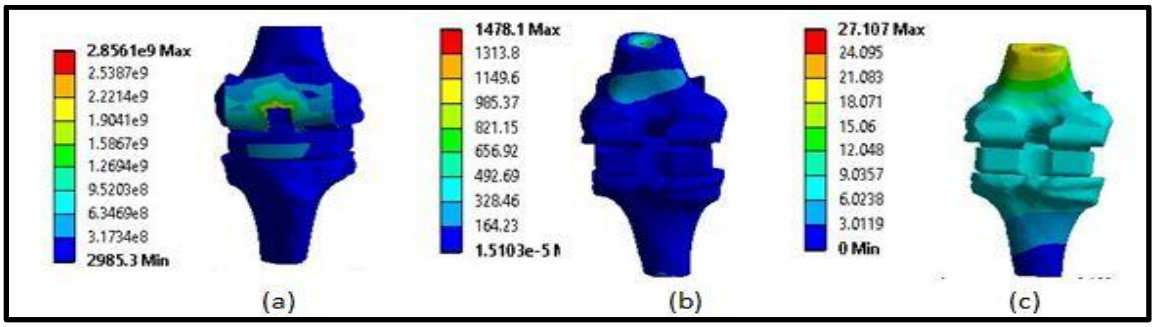

(iv)

Figure 4.11 Static analysis of the knee implant with bone using ZrO_2 at loading conditions of (i) 700 N, (ii) 1000 N, (iii) 1500 N, (iv) 2000 N

Figure 4.11(i-(a)) the stress analysis of knee implant with bone when 700 N of force is applied. The ZrO_2 posse maximum stress of 9.99×10^8 Pa and minimum stress of 1044.8 Pa. Similarly, **Figure 4.11(i-(b))** the strain analysis of the knee implant with bone. The maximum strain of 517.32 and minimum strain of 5.2862×10^{-6} is observed in the ZrO_2. Similarly, **Figure 4.11(i-(c))** represent the total deformation analysis of the knee implant with bone. The total deformation of knee implant with bone maximum value is 9.875 m.

Figure 4.11(ii-(a)) the stress analysis of knee implant with bone when 1000 N of force is applied. The ZrO_2 posse maximum stress of 14.28×10^8 Pa and minimum stress of 1492.7 Pa. Similarly, **Figure 4.11(ii-(b))** the strain analysis of the knee implant with bone. The maximum strain of 739.03 and minimum strain of 7.5517×10^{-6} is observed in the ZrO_2. Similarly, **Figure 4.11(ii c))** represents the total deformation analysis of the knee implant with bone. The total deformation of knee implant with bone maximum value is 13.554 m.

Figure 4.11(iii-(a)) the stress analysis of knee implant with bone when 1500 N of force is applied. The ZrO_2 posse maximum stress of 21.4×10^8 Pa and minimum stress of 2239 Pa. Similarly, **Figure 4.11(iii-(b))** the strain analysis of the knee implant with bone. The maximum strain of 1108.5 and minimum strain of 11.32×10^{-6} is observed in the ZrO_2. Similarly, **Figure 4.11(iii-(c))** represents the total deformation analysis of the knee implant with bone. The total deformation of knee implant with bone maximum value is 20.33 m.

Figure 4.11(iv-(a)) the stress analysis of knee implant with bone when 2000 N of force is applied. The ZrO_2 posse maximum stress of 28.562×10^8 Pa and minimum stress of 2985.3 Pa. Similarly, **Figure 4.11(iv-(b))** the strain analysis of the knee implant with bone. The maximum strain of 1478.1 and minimum strain of 15.1×10^{-6} is observed in the ZrO_2. Similarly, **Figure 4.11(iv-(c))** represents the total deformation analysis of the knee implant with bone. The total deformation of knee implant with bone maximum value is 27.107 m.

The structural analysis of the knee joint has a great importance, as the analytical results provide better information about the mechanical performance of the knee implant. Performing stress analysis using a simulation method instead of intrusive methods is one of the important parts of biomechanical study for different 3D models. Use of an FEM tool such as ANSYS ensured proper and specific definitions of preprocessing conditions for the analysis. The finite element method has been carried out in ANSYS 15.0 software to find out eq. stress, total deformation and eq. strain for various biomaterials for different conditions explained. A knee implant without bone was used in this static analysis. ZrO_2 shows peak eq. stress of 736.52 MPa which is lower than the other implant materials. Ti6Al4V alloy rank second with maximum stress value of 708.04 MPa, 316L SS ranks third with peak stress value of 686.4 MPa. From the results of FEM analysis when knee is in a straight position **(Table 4.1, 4.2, 4.3 and 4.4)**, eq. stress continuously increases at increasing loads of 700 N to 2000 N. The eq. stresses are varying from 343 to 982 MPa at the load 700 N to 2000 N and are maximum varying for ZrO_2. At the steady state condition, total deformation is higher in ZrO_2 than Ti6Al4V alloy and 316L SS. The eq. strain for different implant materials is nearly same there are minor differences in eq. strain value between all implant materials. 316L SS alloy shows peak eq. strain of 9.4975 which is lower than the other implant materials. ZrO_2 ranks second with maximum strain value of 1.62421×10^{-3}. Ti6Al4V alloy ranks third with peak eq. strain value of 0.00029096 and Co-Cr alloy comes last with a peak strain value of 0.0000988. Maximum eq. stress and strain that prosthesis experienced when knee was in a straight position were below permissible stress limit of all biomaterials used.

The transient analysis of the knee joint has a great importance, as the analytical results provide us better information about the mechanical performance of the knee. Performing eq. stress analysis using simulation method instead of intrusive methods is one of the important parts of biomechanical study for different 3D models. Use of an FEM tool such as ANSYS ensured proper and specific definitions of preprocessing conditions for the analysis. It has been established that the angular stability of the knee implant can be improved through this analytical approach. From the stress distribution patterns of the implant, it is clear that there is a concentration of stress around the central portions of the

implant. The three parts of the implant are inspected separately, i.e., the top or femoral part, the middle or lubricating layer and the bottom or tibial part. The top or femoral part shows the maximum concentration of stress at the center of the epicondyle regions. The sandwiched lubricating middle layer shows a maximum stress concentration on the top face. For the bottom or tibial part maximum stress is built up around the region where the stem connected to the base. The current analysis suggests that the central regions of the implant are more prone to wear. Using the above-described method, the grid independence of the analysis was confirmed. Since most of the tabulated results for **(Table 4.5, 4.6 and 4.7)** are of comparable value, it can be said that analysis is grid independent. **Table 4.6** values show a significant deviation from the earlier values. It may be explained by the fact that due to the small value of the time step the analysis did not reach 100% of the solution time. The grid independence proves that using a higher sized meshing also gives a resultant stress, strain and deformation distribution comparable to that obtained from lower sized meshing. Also, time step can be kept higher while solving for the same input conditions. Thus, in the future analysis a coarse mesh size and higher time step can be used to perform analysis on complex geometries, thus reducing the time taken to arrive at the solution.

A knee implant with bone was used in this static analysis. Ti6Al4V alloy shows the peak eq. stress of 1036 MPa which is lower than the other implant materials. ZrO_2 ranks second with maximum stress value of 999 MPa, Co-Cr alloy ranks third with peak stress value of 980.63 MPa and 316L SS comes last with a peak stress value of 962.1 MPa. From the results of FEM analysis when the knee is in a straight position in the **(Table 4.8, 4.9, 4.10 and 4.11**), eq. stress are continuous increases at varying load of 700 N to 2000 N. The eq. stresses are varying from 10.36 to 29.622 MPa at the load 700 to 2000 N and are maximum varying for Ti6Al4V alloy. At the steady state condition, total deformation is higher of Ti6Al4V alloy and ZrO_2 and comparatively less in 316L SS and Co-Cr alloy. The eq. strain for different implant materials is nearly same. There is a minor difference in eq. strain value between all implant materials. Co-Cr alloy shows peak eq. strain of 793.03 m which is lower than the other implant materials. Maximum

eq. stress and strain that prosthesis experienced when the knee was in a straight position were below permissible stress limit of all biomaterials used.

Chapter 5

Conclusion and Future work

CONCLUSION

The static structural and transient analysis of a knee joint with and without bone have great importance as these analytical outcomes provide us with an extensive set of information about the mechanical behavior of the knee joint. The performing eq. stress, eq. strain and total deformation analysis were determined by a simulation process rather than the use of invasive methods. This simulation process is an important part of the biomechanical study of any 3D model. The investigation was carried out by ANSYS 15.0 which assured that only desired and distinct components of the knee implant were involved in the design and analysis of the model. Thus, it has been illustrated that this study paves the way for the embodiment of various biomaterials for use in prostheses joints based on the several parameters. Throughout the study, the most significant criterion to control the geometry of the movement is given and the progressive convergence approach is explained. All hypotheses used in other comparable investigations were performed to save processing time condition and to avoid convergence problems. The hypotheses made in this study are only for data or criterion, and hence are not defined completely. The significant contribution of the current work is to be able to simulate the full articulation using 3D solid design and importing implant material properties to find out the best outcome.

FUTURE WORK

The experimental work on the manufacture of the knee implant can be performed. This will give a correct approach for fabrication of implant in less no of experiments in a cost-effective manner.

REFERENCES

1. Claudon B., Poussel M., Billon-Grumillier C., Beyaert C., and Paysant J., *Knee kinetic pattern during gait and anterior knee pain before and after rehabilitation in patients with patellofemoral pain syndrome.* Gait and Posture, 2012. **36**(1): p. 139-143.
2. Hirschmann M.T., Testa E., Amsler F., and Friederich N.F., T*he unhappy total knee arthroplasty (TKA) patient: higher WOMAC and lower KSS in depressed patients prior and after TKA*. Knee Surgery, Sports Traumatology, Arthroscopy, 2013. **21**(10): p. 2405-2411.
3. Bonnin M., Amendola N.A., Bellemans J., MacDonald S.J., and Menetrey J., T*he knee joint: surgical techniques and strategies*. 2013: Springer Science and Business Media.
4. Kubíček M. and Florian Z., *Stress-strain analysis of knee joint.* Engineering Mechanics, 2009. **16**(5): p. 315-322.
5. Lee J.-N., Chen H.-S., Luo C.-W., and Chang K.-Y., R*apid prototyping and multi-axis NC machining for the femoral component of knee prosthesis.* Life Science Journal, 2010. **7**(1): p. 79-83.
6. Lesso-Arroyo R., Jiménez J.C.S., Castro R.R., and Lopez F.B., *Biomechanical Behavior of the Knee Joint Using ANSYS,* International ANSYS Conference Proceedings, 2004. p. 24-26.
7. Mootanah R., Imhauser C., Reisse F., Carpanen D., Walker R., Koff M., *Development and validation of a computational model of the knee joint for the evaluation of surgical treatments for osteoarthritis.* Computer Methods in Biomechanics and Biomedical Engineering, 2014. **17**(13): p. 1502-1517.
8. Peña E., Del Palomar A.P., Calvo B., Martínez M., and Doblaré M., *Computational modeling of diarthrodial joints. Physiological, pathological and pos-surgery simulations*. Archives of Computational Methods in Engineering, 2007. **14**(1): p. 47-91.

9. Van Jonbergen H.-P.W., Innocenti B., Gervasi G.L., Labey L., and Verdonschot, *Differences in the stress distribution in the distal femur between patellofemoral joint replacement and total knee replacement: a finite element study*. Journal of Orthopaedic Surgery and Research, 2012. **7**(1): p. 1.
10. Pena E., Calvo B., Martinez M., Palanca D., and Doblare M., *Influence of the tunnel angle in ACL reconstructions on the biomechanics of the knee joint.* Clinical Biomechanics, 2006. **21**(5): p. 508-516.
11. Beynnon B. and Amis A.A., *In vitro testing protocols for the cruciate ligaments and ligament reconstructions. Knee Surgery,* Sports Traumatology, Arthroscopy, 1998. **6**(1): p. S70-S76.
12. Machado M., Flores P., Claro J.P., Ambrósio J., Silva M., Completo A., *Development of a planar multibody model of the human knee joint. Nonlinear Dynamics,* 2010. **60**(3): p. 459-478.
13. Nieuwenhuijse M.J., Nelissen R., Schoones J., and Sedrakyan A., *Appraisal of evidence base for introduction of new implants in hip and knee replacement: a systematic review of five widely used device technologies.* 2014.
14. Winter D.A., *Biomechanics and motor control of human movement.* 2009: John Wiley & Sons.
15. Westervelt E.R., Buche G., and Grizzle J.W., *Experimental validation of a framework for the design of controllers that induce stable walking in planar bipeds*. The International Journal of Robotics Research, 2004. **23**(6): p. 559-582.
16. Paul A.J., Slavens B.A., Graf A., Krzak J., Vogel L., and Harris G.F. *Upper extremity biomechanical model for evaluation of pediatric joint demands during wheelchair mobility.* in Engineering in Medicine and Biology Society (EMBC), 2012 Annual International Conference of the IEEE. 2012: IEEE.
17. Kawakami S., Kodama N., Maeda N., Sakamoto S., and Minagi S., *A new posture measurement method for measuring intrinsic standing posture.* CRANIO, 2014. **32**(2): p. 98-103.

18. K.E. Moglo, *On the coupling between anterior and posterior cruciate ligaments, and knee joint response under anterior femoral drawer in flexion: a finite element study.* Clinical Biomechanics, 2003. **18**: p. 751-759.
19. Lee J.N., Lee R.S., and Chang K.Y. *Geometric Modeling and Multi-Axis NC Machining for Custom-Made Femoral Stem*. Advanced Materials Research, 2011. **264**, p. 1619-1624.
20. Ferreira P., Relvas C., and Simões F. *Analysis of machining operations of a femoral prosthesis using CAM applications*. Key Engineering Materials, 2013. **554**, p.2029-2037.
21. Qiu T.-X., Teo E.-C., Yan Y.-B., and Lei W., *Finite element modeling of a 3D coupled foot–boot model*. Medical Engineering and Physics, 2011. **33**(10): p. 1228-1233.
22. Knopf E., *Analysis of biomechanical effectiveness of valgus-inducing knee brace for osteoarthritis of knee.* Journal of Rehabilitation Research and Development, 2010. **47**(5): p. 419.
23. Saurabh A.Y., and B.R Rawal, B*iomechanical Analysis of Different Knee Prosthesis Biomaterials Using Fem*. IOSR Journal of Mechanical and Civil Engineering (IOSR-JMCE), May- Jun. 2014 **11**(3): p. 120-128.
24. Weinans H., Huiskes R., and Grootenboer H. J., *The behavior of adaptive bone-remodeling simulation models.* Journal of Biomechanics, 1992. **25**(12): p. 1425-1441.
25. Mommersteeg T., Huiskes R., Blankevoort L., Kooloos J., Kauer J., and Maathuis, *A global verification study of a quasi-static knee model with multi-bundle ligaments.* Journal of Biomechanics, 1996. **29**(12): p. 1659-1664.
26. Piazza S.J. and Delp S.L., *Three-dimensional dynamic simulation of total knee replacement motion during a step-up task*. Journal of Biomechanical Engineering, 2001. **123**(6): p. 599-606.
27. Liau J.-J., Cheng C.-K., Huang C.-H., and Lo W.-H., T*he effect of malalignment on stresses in polyethylene component of total knee prostheses–a finite element analysis.* Clinical Biomechanics, 2002. **17**(2): p. 140-146.

28. Bankoff A.D.P., B*iomechanical characteristics of the bone*. 2012: Intech Open Access Publisher.
29. Erickson G.M., Catanese J., and Keaveny T.M., *Evolution of the biomechanical material properties of the femur.* The Anatomical Record, 2002. **268**(2): p. 115-124.
30. Imbert L., Aurégan J.-C., Pernelle K., and Hoc T., *Microstructure and compressive mechanical properties of cortical bone in children with osteogenesis imperfecta treated with bisphosphonates compared with healthy children*. Journal of the Mechanical Behavior of Biomedical Materials, 2015. **46**: p. 261-270.
31. Taksali S., Grauer J.N., and Vaccaro A.R., *Material considerations for intervertebral disc replacement implants.* The Spine Journal, 2004. **4**(6): p. S231-S238.
32. Sivaraj P. and Rajeshkumar G., *Prediction of Mechanical Properties of Hybrid Fiber Reinforced Polymer Composites.* International Journal Of Engineering Research (ISSN: 2319-6890)(Online): p. 2347-5013.
33. Burkhart T.A., Andrews D.M., and Dunning C.E., *Finite element modeling mesh quality, energy balance and validation methods: A review with recommendations associated with the modeling of bone tissue.* Journal of Biomechanics, 2013. **46**(9): p. 1477-1488.
34. Cornelissen J.T., Taghipour F., Escudié R., Ellis N., and Grace J.R., *CFD modeling of liquid–solid fluidized bed*. Chemical Engineering Science, 2007. **62**(22): p. 6334-6348.
35. Aula A., Akmeliawati R., Ahmad S., Altalmas T., and Sidek S.N. Integrated Design, *Modeling and Analysis of Two-wheeled Wheelchair for Disabled*. in Proc. 16th Int. Conf. on Climbing and Walking Robots (Sidney, Australia). 2013.
36. St-Onge N., Chevalier Y., Hagemeister N., Van De Putte M., and De Guise J., *Effect of ski binding parameters on knee biomechanics: a three-dimensional computational study.* Medicine and Science in Sports and Exercise, 2004. **36**(7): p. 1218-1225.

37. Malla R.B. and Gionet T.G., *Dynamic response of a pressurized frame-membrane lunar structure with regolith cover subjected to impact load.* Journal of Aerospace Engineering, 2011. **26**(4): p. 855-873.